UNIVERSITAT POLITÈCNICA DE CATALUNYA
BARCELONATECH
Escola d'Enginyeria de Barcelona Est


Politecnico di Torino

Master's Degree in Energy and Nuclear Engineering

Universitat Politècnica de Catalunya Barcelonatech – Escola D'enginyeria de Barcelona Est

Erasmus Mundus Master's Degree in Hydrogen Systems and Enabling Technologies (HySET)

A simulation-based evaluation of a direct air capture system with coupled electrochemical and thermochemical processes

Master Thesis Report

Academic and Industrial Supervisors:
Prof. Massimo Santarelli (PoliTO)
Prof. Ignasi Burgués-Ceballos (UPC)
Gerald Sprachmann (*Shell*)

Candidate:
Giuseppe Calabrese

June 2025

This page intentionally left blank

Preface

This thesis project, *A simulation-based evaluation of a direct air capture system with coupled electrochemical and thermochemical processes*, which represents more than just research, marks the final milestone of my journey within the HySET program and has been developed during a six-month internship at the Energy Transition Campus Amsterdam (ETCA), hosted by *Shell*. Before delving into the details of this work, I would like to take a moment to express my genuine gratitude to those who have supported and guided me throughout this journey.

I am deeply grateful for the unique opportunities the HySET program has offered me – both academically and personally – and I could not have envisioned a more enriching way to conclude this experience. I would like to express my sincere gratitude to the HySET consortium for making this path possible, and in particular to Evren Unsal, Academic Partnership Manager at *Shell*, whose dedication and effort enabled HySET students to carry out their internship at *Shell*. Without her, this experience would not have been possible.

My heartfelt thanks go to my industrial and academic supervisors: Gerald Sprachmann from *Shell*, for giving me the opportunity to work on this project and for his outstanding and continuous guidance throughout its development; Prof. Massimo Santarelli from Politecnico di Torino and Prof. Ignasi Burgués-Ceballos from Universitat Politècnica de Catalunya, for their insightful feedback, expertise and encouragement which were instrumental in shaping the work.

A warm thank you goes to all the colleagues at *Shell* with whom I had the pleasure of interacting and exchanging ideas. Each conversation has been a source of learning and inspiration. I am grateful for the professional and welcoming environment at ETCA, which allowed me to growth both as a professional and as a person.

I am also thankful to my friends and family, who – even from afar – provided unwavering support and motivation throughout this period. Finally, a special thank you to my fellow interns, who shared this chapter of the journey with me and made the experience lighter, richer, and full of memorable moments.

Giuseppe Calabrese
Amsterdam, June 2025

Abstract

As the climate change has become more pronounced, the limitations around mitigation strategies such as renewable energy deployment and energy efficiency improvements are becoming more visible. While these approaches are indispensable, they are unlikely to achieve the full-scale decarbonization required to meet global climate targets alone. Consequently, technologies that actively remove carbon dioxide from the atmosphere, known as Negative Emission Technologies (NETs), are gaining recognition as essential components of a comprehensive and across-the-board climate strategy.

This study focuses on Direct Air Capture (DAC) technology, one of the NETs. A novel system for CO_2 capture from the atmosphere that integrates electrochemical and thermochemical processes is studied. The system captures CO_2 using an aqueous NaOH solution, regenerates the sorbent electrochemically via Na_2CO_3 electrolysis, and releases CO_2 through the thermochemical decomposition of $NaHCO_3$. The process offers three key advantages: it produces valuable by-products such as hydrogen and oxygen; it relies primarily on electricity, facilitating integration with renewable energy sources; and it requires only low-temperature heat, enabling effective coupling with waste heat recovery solutions.

The system was modeled using *Aspen Plus* and designed to support a CO_2 methanation process for synthetic natural gas (SNG) production, taking advantage of the combined CO_2 and H_2 production. The simulation aimed to assess the energy demand of the process and identify key operational and design parameters.

A preliminary techno-economic evaluation was conducted to estimate the CO_2 capture cost of the process and assess the economic viability of the system. The analysis explored the influence of economic parameters and components cost, with particular attention to the benefits of hydrogen co-production. The findings contribute to a broader understanding of how integrated DAC technologies can support scalable and cost-effective carbon removal, especially in applications where both CO_2 and H_2 are valuable inputs.

Sommario

Con il cambiamento climatico sempre più evidente, emergono i limiti delle strategie di mitigazione come l'adozione di energie rinnovabili e il miglioramento dell'efficienza energetica. Sebbene siano fondamentali, queste misure da sole difficilmente porteranno alla decarbonizzazione su larga scala necessaria per raggiungere gli obiettivi climatici globali. Di conseguenza, le tecnologie che rimuovono attivamente l'anidride carbonica dall'atmosfera, note come Tecnologie a Emissioni Negative (NET), stanno acquisendo importanza come elementi essenziali di una strategia climatica completa e trasversale.

Questo studio si concentra sulla tecnologia di Cattura Diretta dell'Aria (DAC), una delle NET. Viene analizzato un sistema innovativo per la cattura di CO_2 dall'atmosfera che integra processi elettrochimici e termochimici. Il sistema cattura CO_2 utilizzando una soluzione acquosa di NaOH, rigenera l'assorbente elettrochimicamente tramite elettrolisi di Na_2CO_3 e rilascia CO_2 attraverso la decomposizione termochimica di $NaHCO_3$. Il processo presenta tre vantaggi principali: produce sottoprodotti di valore come idrogeno e ossigeno; si basa principalmente sull'elettricità, facilitando l'integrazione con fonti rinnovabili; e richiede solo calore a bassa temperatura, permettendo l'integrazione con sistemi di recupero del calore di scarto.

Il sistema è stato modellato con *Aspen Plus* e progettato per supportare un processo di metanazione della CO_2 per la produzione di gas naturale sintetico (SNG), sfruttando la produzione combinata di CO_2 e H_2. La simulazione ha valutato il fabbisogno energetico del processo e identificato i parametri chiave di progettazione e operativi.

È stata condotta una valutazione tecnico-economica preliminare per stimare il costo di cattura della CO_2 e valutare la fattibilità economica del sistema. L'analisi ha esplorato l'influenza dei parametri economici e dei costi dei componenti, con particolare attenzione ai benefici della coproduzione di idrogeno. I risultati contribuiscono a una comprensione più ampia di come le tecnologie DAC, integrate con la produzione di idrogeno, possano supportare un processo di decarbonizzazione scalabile ed economicamente sostenibile, specialmente in applicazioni in cui CO_2 e H_2 sono risorse preziose.

Resum

A mesura que el canvi climàtic es fa més evident, les limitacions de les estratègies de mitigació com la implantació d'energies renovables i la millora de l'eficiència energètica esdevenen més evidents. Tot i que són imprescindibles, aquestes mesures difícilment assoliran per si soles la descarbonització a gran escala necessària per complir els objectius climàtics globals. En conseqüència, les tecnologies que eliminen activament el diòxid de carboni de l'atmosfera, conegudes com a Tecnologies d'Emissions Negatives (NET), estan guanyant reconeixement com a agents essencials d'una estratègia climàtica integral.

Aquest estudi se centra en la tecnologia de Captura Directa de l'Aire (DAC), una de les NET. S'estudia un sistema innovador per a la captura de CO_2 de l'atmosfera que integra processos electroquímics i termoquímics. El sistema captura CO_2 mitjançant una solució aquosa de NaOH, regenera l'absorbent electroquímicament mitjançant electròlisi de Na_2CO_3 i allibera CO_2 a través de la descomposició termoquímica de $NaHCO_3$. El procés ofereix tres avantatges clau: produeix subproductes valuosos com hidrogen i oxigen; es basa principalment en electricitat, facilitant la integració amb fonts renovables; i només requereix calor a baixa temperatura, permetent la integració amb sistemes de recuperació de calor residual.

El sistema s'ha modelat amb *Aspen Plus* i s'ha dissenyat per donar suport a un procés de metanació de CO_2 per a la producció de gas natural sintètic (SNG), aprofitant la producció combinada de CO_2 i H_2. La simulació ha avaluat la demanda energètica del procés i ha identificat els paràmetres clau de disseny i operació.

S'ha dut a terme una avaluació tecnoeconòmica preliminar per estimar el cost de captura de CO_2 i avaluar la viabilitat econòmica del sistema. L'anàlisi explora la influència dels paràmetres econòmics i el cost dels components, amb especial atenció als beneficis de la coproducció d'hidrogen. Els resultats contribueixen a una comprensió més àmplia de com les tecnologies DAC integrades poden donar suport a una eliminació de carboni escalable i rendible, especialment en aplicacions on tant el CO_2 com l'H_2 són recursos valuosos.

Resumen

A medida que el cambio climático se intensifica, las limitaciones de las estrategias de mitigación como el despliegue de energías renovables y la mejora de la eficiencia energética se hacen más evidentes. Aunque son fundamentales, estas medidas difícilmente lograrán por sí solas la descarbonización a gran escala necesaria para alcanzar los objetivos climáticos globales. En consecuencia, las tecnologías que eliminan activamente dióxido de carbono de la atmósfera, conocidas como Tecnologías de Emisiones Negativas (NET), están ganando reconocimiento como actores esenciales de una estrategia climática integral.

Este estudio se centra en la tecnología de Captura Directa del Aire (DAC), una de las NET. Se analiza un sistema novedoso para la captura de CO_2 atmosférico que integra procesos electroquímicos y termoquímicos. El sistema captura CO_2 mediante una solución acuosa de NaOH, regenera el absorbente electroquímicamente mediante electrólisis de Na_2CO_3 y libera CO_2 a través de la descomposición termoquímica de $NaHCO_3$. El proceso ofrece tres ventajas clave: produce subproductos valiosos como hidrógeno y oxígeno; se basa principalmente en electricidad, lo que facilita su integración con fuentes renovables; y requiere solo calor de baja temperatura, lo que permite su acoplamiento con soluciones de recuperación de calor residual.

El sistema ha sido modelado con *Aspen Plus* y diseñado para apoyar un proceso de metanación de CO_2 para la producción de gas natural sintético (SNG), aprovechando la producción combinada de CO_2 y H_2. La simulación tiene como objetivo evaluar la demanda energética del proceso e identificar parámetros clave de operación y diseño.

Se ha realizado una evaluación tecnoeconómica preliminar para estimar el coste de captura de CO_2 y analizar la viabilidad económica del sistema. El análisis explora la influencia de los parámetros económicos y el coste de los componentes, con especial atención a los beneficios de la coproducción de hidrógeno. Los resultados contribuyen a una comprensión más amplia sobre cómo las tecnologías DAC integradas pueden apoyar una eliminación de carbono escalable y rentable, especialmente en aplicaciones donde tanto el CO_2 como el H_2 son recursos valiosos.

List of Acronyms

APEA	Aspen process economic analyzer
BEC	Bare erected cost
BFD	Block flow diagram
BoP	Balance of plant
BPMED	Bipolar membrane electrodialysis
C&OC	Contingencies and owner's costs
CAPEX	Capital expenditure
CCF	Capital charge factor
CCS	Carbon capture and storage
CCU	Carbon capture and utilization
CE	Carbon engineering
DAC	Direct air capture
eCCC	Electrochemical carbon capture and concentration
EMAR	Electrochemically mediated amine regeneration
EPC	Engineering procurement and construction
ETCA	Energy transition campus Amsterdam
GHG	Greenhouse gas
HER	Hydrogen evolution reaction
IC	Indirect cost
MOFs	Metal-organic frameworks
NET	Negative emissions technology
NETL	National energy technology laboratory
O&M	Operation and maintenance
OER	Oxygen evolution reaction
OPEX	Operational expenditure
PFD	Process flow diagram
ppm	Parts per million
RES	Renewable energy source
RH	Relative humidity
SDG	Sustainable development goals
SNG	Synthetic natural gas
SS	Stainless steel
TDPC	Total direct plant cost
TIC	Total installation cost
TOC	Total overnight capital
TREMP™	Topsøe Recycle Energy-efficient Methanation Process
TRL	Technology readiness level

Table of Contents

PREFACE I

ABSTRACT II

SOMMARIO III

RESUM IV

RESUMEN V

LIST OF ACRONYMS VI

TABLE OF CONTENTS VII

LIST OF FIGURES IX

LIST OF TABLES X

1. INTRODUCTION 1

1.1. Research motivation 1

1.2. Research objectives 2

1.3. Structure of the report 3

2. LITERATURE REVIEW 4

2.1. Fundamentals of DAC processes 4

2.1.1. Liquid-sorbent-based DAC 5

2.1.2. Solid-sorbent-based DAC 6

2.1.3. Membrane-based DAC 8

2.1.4. Electrochemical-based DAC 9

2.2. DAC cost 10

2.3. *Obrist* DAC 11

3. METHODOLOGY 13

3.1. Heuristics and assumptions 13

3.2. System modeling 15

3.2.1. Air-contactor subsystem 16

3.2.2. Na_2CO_3 electrolysis subsystem 18

3.2.3. $NaHCO_3$ thermochemical decomposition subsystem 19

3.2.4. NaOH concentration subsystem 20

3.2.5. NaOH/Na_2CO_3 separation subsystem 21

3.2.6. Water balance 21

3.3. System sizing 21
3.4. Preliminary economic analysis 22
3.4.1. Capital expenditures 22
3.4.2. Operational expenditures 23
3.4.3. Capture cost 23

4. RESULTS AND DISCUSSION 24
4.1. System modeling results 24
4.1.1. Process specific energy consumption 27
4.1.2. Water losses 29
4.2. System sizing results 29
4.2.1. Air-contactor sizing 30
4.2.2. Na_2CO_3 electrolysis cell sizing 32
4.3. Economic analysis results 33
4.3.1. Total overnight capital 34
4.3.2. Operation and maintenance costs 35
4.3.3. Capture Cost 37
4.3.4. Adjusted capture cost accounting for H_2 revenue 38
4.3.5. Impact of parameters variation on capture cost 39
4.4. Comparison with other DAC processes 42

5. CONCLUSIONS 46

APPENDIX A – PFD OF THE PROCESS WITH THE SUBSYSTEMS HIGHLIGHTED 48

APPENDIX B – STREAMS TABLE 49

APPENDIX C – DESIGN SPECIFICATIONS OF CONVENTIONAL EQUIPMENT 51

APPENDIX D – CONVETIONAL PROCESS EQUIPMENT COST 52

ANNEX I – SUSTAINABILITY REPORT 53
I.I Environmental sustainability 53
I.II Economic sustainability 54
I.III Ethical implications 55
I.IV Relationship with the SDGs 55

REFERENCES 56

List of Figures

Figure 2.1 Block flow diagram of the system under study _____ 12

Figure 3.1 Process route for CO_2 methanation combining DAC, RES, and renewable hydrogen. The boundaries of the analysis of this thesis work are delineated by a solid red line14

Figure 3.2 Process flow diagram of the Aspen Plus developed model _____ 17

Figure 4.1 Specific energy consumption of the DAC process _____ 28

Figure 4.2 Conceptual design of the air-contactor unit, illustrating its overall geometry and modular configuration [51] _____ 32

Figure 4.3 Adjusted capture cost response to changes in electricity price, Na_2CO_3 electrolysis installation cost, CCF and H_2 market price _____ 42

Figure 4.4 Capture cost of the three processes compared under harmonized conditions 45

List of Tables

Table 3.1 Overview of the inlet air feed composition used in the Aspen Plus simulation 15

Table 4.1 Equipment list 30

Table 4.2 Methodology for the calculation of the TOC from NETL [52], [53] 34

Table 4.3 TOC for the four subsystems 35

Table 4.4 Summary of utility consumption for the DAC process, reported per ton of CO_2 captured and on an annual basis 35

Table 4.5 Annual variable operational and maintenance costs based on utility consumption and unit prices 37

Table 4.6 Breakdown of TOC, levelized fixed and variable O&M costs, and CO_2 capture cost per subsystem 37

Table 4.7 Breakdown of TOC, levelized fixed and variable O&M costs, and CO_2 capture cost per subsystem, including revenues from H_2 selling 39

Table 4.8 Specific energy demand for the three processes under comparison 44

1.Introduction

1.1. Research motivation

Climate change represents one of the most pressing challenges of the twenty-first century, with significant implications for ecosystems, economies, and lives both directly and indirectly, through undermining the environmental and social determinants of health [1]. Rapid action to decarbonize industrial practices, economies and build resilience is justified on health, human rights, environmental and economic grounds. Emission of greenhouse gas (GHG) , such as carbon dioxide (CO_2), methane (CH_4), and nitrous oxide (N_2O) are linked to human activities. Due to the combustion of fossil fuels for energy generation and transport, agriculture and industrial processes, the GHG emissions have been contributing to the increase in global temperatures in the atmosphere [2].

With the 2015 Paris Agreement, 196 Parties at the UN Climate Change Conference (COP21) in Paris, France, agreed to commit themselves to *stabilizing the global average temperature to well below 2℃ above pre-industrial levels and pursuing efforts to limit the temperature increase to 1.5℃ above pre-industrial levels [3], [4]*. Since then, many countries around the globe have been making a coordinated effort to decarbonize.

CO_2 is the most dominant GHG produced by the burning of fossil fuels, industrial production, and land usage. The concentration of CO_2 has been reported to have increased to $420\ ppm$ today, from $280\ ppm$ in 1750, and continuous increase is anticipated if the problem of CO_2 emissions is not properly addressed in the coming years [5].

Decarbonization – defined as the process of reducing carbon emissions across energy, industrial, and transport sectors – has emerged as one of the main strategies to address climate change [6]. Research suggests that preventive methods, consisting of the promotion of renewable energy sources and energy efficiency programs, will not be sufficient to achieve the required reductions of CO_2 in the coming decades, and remediation methods, such as technologies aiming at reducing or capturing the emitted CO_2 are required. Furthermore, it is also suggested that remediation methods alone will not be enough to meet the targets, especially the one set by the Paris Agreement, and negative emissions technologies (NETs) – technologies that can directly remove CO_2 from the atmosphere – will be necessary [7].

Carbon capture refers to technologies that directly capture the CO_2 that is emitted during the industrial operations and/or in the power generation plants, with the aim of lowering the concentration of CO_2 in the flue gases before releasing them into the atmosphere. The captured CO_2 can then either be permanently stored underground or reutilized for other purposes, such as in the production of fuels or other valuable chemical products. Carbon capture and storage (CCS) represents a long-term solution, continuously reducing CO_2 emissions, while carbon capture and utilization (CCU) is considered more of a short-term solution, as the captured CO_2 is reutilized to produce other feedstocks. CCU is seen as complementary to CCS, with the ultimate goal being the elimination of CO_2 through permanent storage.

The direct air capture (DAC), one of the NETs, is the extraction of CO_2 directly from ambient air [8]. It is one of the solutions that has received interest in the last decades. Different from the already deployed carbon capture technologies for the reduction of the point source emissions, DAC has also the potential to address emissions from distributed sources and can be utilized in principle for both CCU or CCS solutions in the short and long run scenarios, respectively.

1.2. Research objectives

This thesis project focuses on the evaluation of a specific DAC technology proposed by *Obrist [9], [10]*. The CO_2 capture process, which utilizes a liquid solvent, makes use of coupled electrochemical and thermochemical processes to regenerate the solvent, release the captured CO_2 and produce useful by-products (hydrogen (H_2) and oxygen (O_2)). Economically, the process is claimed to be more advantageous compared to other DAC approaches due to its primary reliance on electricity, which enables integration with low-cost renewable sources, and its low-temperature thermal energy demand, which allows for coupling with waste heat recovery solutions.

The primary objective of this project is to develop a deeper understanding of *Obrist* DAC technology. This will be achieved by evaluating the energy consumption throughout the capture process and assessing the associated costs. The energy consumption will be estimated by modeling the system using *Aspen Plus*, a process simulation software. Additionally, the economic feasibility of the process will be quantified through a preliminary analysis, which will evaluate both the capital expenditure (CAPEX) and operational expenditure (OPEX) of the technology, with the aim of estimating the capture cost of the DAC process.

1.3. Structure of the report

The next chapter of this report presents a literature review of existing DAC technologies, focusing on their principles, advantages, limitations and current challenges. The subsequent chapter details the methodology employed in this study, including a description of the model developed using the *Aspen Plus* software for the DAC system, as well as the heuristics and assumptions made. This chapter also outlines the approach adopted for data collection and generation of results. The main findings of the analysis are presented in the results and discussion chapter. Finally, the conclusion chapter provides a summary of the key observations, addresses the issues that have been resolved, identifies those that remain unresolved, and offers suggestions for potential future research directions to further explore the topic.

2.Literature Review

Point-source CO_2 capture, as a solution for limiting the impact of CO_2 emissions, is a well-established technology employed to reduce the CO_2 concentration in the flue gases of industrial or energy production plants [11]. By targeting these high-emission points, substantial reductions in overall CO_2 emissions may be achieved. But, it has already been proven that this solution alone will not be sufficient to meet the targets set in terms of climate change and decarbonization, such as limiting the increase in the average global temperature to $1.5℃$ [12]. Therefore, the implementation of new NETs in the coming decades will be crucial. However, all these technologies are still in the demonstration phase (TRL 7), mainly due to techno-economic barriers that hinder their development. These barriers will need to be quickly overcome if these technologies are to reach the commercialization level (TRL 9) and be effectively implemented in the near future [13].

DAC technologies have been amongst the most investigated NETs in recent years. In this chapter, the primary DAC technologies reported in the literature are discussed. The objective is to provide an overview of the fundamental principles of DAC technologies, current and prospective research trends around them, as well as the limitations and unresolved issues that require further investigation. Additionally, some of the main economic aspects of the technology will be discussed. Finally, the focus will be on describing the DAC technology proposed by *Obrist*, considered as the starting point and main motivation of this thesis work.

2.1. Fundamentals of DAC processes

The majority of the proposed DAC technologies essentially consist of two phases: in the first phase, sometimes referred to as 'loading', the atmospheric air is brought into contact with a sorbent, with the aim of extracting the CO_2 present in the air. In the second phase, 'unloading', a chemical or physical process is employed to regenerate the sorbent and release the previously captured CO_2. Alternative approaches, consisting of merging the two phases into a single step, have recently emerged and are currently being considered as possible alternatives to the already investigated, traditional approaches.

Available technologies can be classified in four groups based on the CO_2 capturing and solvent regeneration methods: liquid-sorbent-based absorption, solid-sorbent-based adsorption, membrane-based, and electrochemical-based DAC. It should be noted that additional alternative approaches to DAC technology, such as mineral carbonation or photocatalytic CO_2

conversion, are discussed in the literature. These methods are still at an early stage of development, therefore, will not be discussed in this report, as they are considered too far from the proposed objectives [14], [15].

2.1.1. Liquid-sorbent-based DAC

Because of the ultra-dilute nature of CO_2 in the atmosphere – today, the concentration of CO_2 in the atmosphere is ca. 400 ppm, roughly 350 times lower than that found in a typical point-source emitter in industry such as refineries or energy production plants [16] – the liquid sorbents with strong CO_2 binding affinity, such as aqueous alkali hydroxide solutions, were historically the first type of sorbent investigated for DAC technologies. Solution of calcium hydroxide ($Ca(OH)_2$) was the very first liquid sorbent employed for DAC technology, when its utilization was conceptualized for the first time in 1999 [17].

In this study, the aqueous alkali hydroxide solution was brought in contact with the atmospheric air, leading to the formation of calcium carbonate ($CaCO_3$), which precipitates and accumulates. $CaCO_3$ was then separated and dried, undergoing the so-called calcination process, to form calcium oxide (CaO) and release the captured CO_2. $Ca(OH)_2$ was then regenerated via hydration, closing the cycle. The overall process can be described by the following set of global reactions (Reactions 2.1–2.3):

$$Ca(OH)_2 + CO_2 \rightarrow CaCO_3 + H_2O \quad \Delta H^o = -109\ kJ/mol \qquad 2.1$$

$$CaCO_3 \rightarrow CaO + CO_2 \quad \Delta H^o = +179.2\ kJ/mol \qquad 2.2$$

$$CaO + H_2O \rightarrow Ca(OH)_2 \quad \Delta H^o = -64.5\ kJ/mol \qquad 2.3$$

The advantage of a strong binding affinity between $Ca(OH)_2$ and CO_2 during the adsorption stage, translates into a disadvantage during the release phase of CO_2 and the regeneration of the sorbent, because of the high amount of energy required. Because of this main drawback, and some other additional problematic aspects, such as the low solubility in water of $Ca(OH)_2$, the research community moved into exploring alternative liquid sorbents and regeneration processes that could be more energy and cost effective. The second largely investigated liquid sorbent employed is solution of sodium hydroxide (NaOH), following the Kraft process, a well-known process for the extraction of cellulose in the pulp and paper industry, employed since 1884 [15], [18]. NaOH still allows for strong binding of CO_2, with an added advantage of being highly soluble in water, and the well-established process could in principle favor the faster development of the technology. In this approach, NaOH is used in the contactor to absorb CO_2

from the atmospheric air, producing sodium carbonate (Na_2CO_3) solution. Na_2CO_3 then reacts with $Ca(OH)_2$, regenerating NaOH and precipitating $CaCO_3$, in a process called causticization. $CaCO_3$ then undergoes the already mentioned calcination process to release the captured CO_2 first and regenerate $Ca(OH)_2$ after. The process can be summarized with the following reactions (Reactions 2.4–2.7):

$$Contactor: 2NaOH + CO_2 \rightarrow Na_2CO_3 + H_2O \quad \Delta H^o = -109.4\ kJ/mol \tag{2.4}$$

$$Causticizer: Na_2CO_3 + Ca(OH)_2 \rightarrow 2NaOH + CaCO_3 \quad \Delta H^o = -5.3\ kJ/mol \tag{2.5}$$

$$Calciner: CaCO_3 \rightarrow CaO + CO_2 \quad \Delta H^o = +179.2\ kJ/mol \tag{2.6}$$

$$Slaker: CaO + H_2O \rightarrow Ca(OH)_2 \quad \Delta H^o = -64.5\ kJ/mol \tag{2.7}$$

However, large energy requirements are present, again due to the presence of the calcination process. Therefore, alternative routes exploiting processes different from the simple thermal decomposition for the regeneration of the solvent and release of the captured CO_2 are currently under research.

2.1.2. Solid-sorbent-based DAC

DAC technologies based on solid material have also been investigated. Typical solid materials, such as carbon-based materials, zeolites, and metal-organic frameworks (MOFs), result in stable structures with easy preparation routes but generally lower adsorption properties when compared to liquid sorbents [19]. Carbon-based materials can be suitable for CO_2 capture because of their ultra-high specific surface area and low cost. However, due to their small adsorption capacity at low CO_2 partial pressure and the weak selectivity towards nitrogen (N_2) and moisture, they have been dismissed as good candidates for CO_2 capture technologies. Zeolites, depending on the alkali cation on the surface, can perform better towards CO_2 adsorption compared to carbon-based materials. However, low CO_2 selectivity poses a major obstacle that hinders the development of these materials for DAC applications. MOFs, emerging new nanocrystalline porous materials, exhibit promising potential for CO_2 capture thanks to their flexibility in composition, surface properties, and pore structure. Despite this, the performance of MOFs in terms of adsorption capacity is highly reduced in the presence of water vapor. Overall, the main drawbacks for solid-sorbent-based CO_2 adsorption lie in the small CO_2 uptake, slow CO_2 sorption kinetics, and decreased selectivity in presence of water vapor [20], [21], [22].

The last class of solid materials investigated for DAC applications consists of modifying the above-mentioned materials to improve performance and address the main encountered drawbacks. Amine-modified solid materials have shown potential for DAC applications, mainly due to their high CO_2 adsorption capacity, fast kinetics, and relatively low energy consumption [23]. This class of materials can be divided into subcategories according to the technique used for their preparation: class 1 adsorbents, class 2 adsorbents, and class 3 adsorbents. These different classes have been developed sequentially to continually improve them and overcome various drawbacks. The choice of amine class influences the adsorption performance and therefore must be made with proper attention. In Class 1 adsorbents, physically impregnated amine-modified materials, the amine groups are only physically adsorbed onto the support through the impregnation method, rather than being chemically bonded. Due to this and the relatively high regeneration temperature (> 100 °C), Class 2 adsorbents, which are chemically grafted amine-modified materials, were proposed to overcome these drawbacks. However, this new class of materials shows lower CO_2 uptake, limiting the application of them for CO_2 capture. Class 3 adsorbents, in-situ polymerized amine-modified materials, were synthetized to overcome the limitations of class 1 and 2 adsorbents. Class 3 adsorbents resulted in easy manufacturing routes, cost-effectiveness, and cyclic stability, but revealed higher energy consumption and cost for regeneration. Therefore, the research community is moving into exploring alternatives for the regeneration of these materials that not necessarily need thermal treatment, and that can therefore be in principle more effective from an economic and energetic point of view.

Modification of MOFs with amines has been proposed as a strategy to enhance the CO_2 adsorption capacity of MOFs by increasing the affinity between the adsorption sites and CO_2 molecules [24]. However, the main disadvantage reported for these amine-MOF composites is their relatively narrow pore size, which hinders the diffusion of amines into their pores and the mass transfer of CO_2 within the pore channels. Another type of composite material investigated is the combination of amines mixed with metal oxides. These materials are considered as a solution to mitigate the relatively slow adsorption kinetics and poor thermal stability by enhancing the properties of the materials used as support for the amino groups, improving morphology, hydrothermal resistance, and binding to amino groups [25].

In conclusion, solid adsorption materials, despite their advantages of easy preparation and stability, are less appealing for DAC applications due to their poor adsorption capacity and the issues related to cyclability, which hinder the development of cost-effective alternatives, when compared to liquid adsorption materials.

2.1.3. Membrane-based DAC

Another approach for DAC technologies, different from the above-mentioned ones in which two distinct steps, 'loading' and 'unloading', can be clearly distinguished, makes use of membranes to directly extract CO_2 from the atmosphere on the retentate side. This method eliminates problems related to the regeneration of the absorbent medium. However, due to the low partial pressure of CO_2 in the atmosphere, which limits the intensity of the driving force for CO_2 permeation through the membranes, the low general CO_2 permeance, and the high energy requirement to set the required pressure difference, the approach received less attention. Despite this, a few researchers have tested the potential of already well-established membrane technologies for DAC applications. Given the general knowledge about membranes, if the mentioned drawbacks can be overcome, membrane-based DAC technologies could become a promising approach in the near future, for faster development of DAC.

An investigated approach consisted of a multistage separation process, in which atmospheric air is blown through a set of identical membranes connected in series to achieve the desired concentration of CO_2, as one single separation stage is insufficient for this purpose [26]. This study allowed researchers to understand the main parameters to be considered when looking at process design and optimization. As a result, it was found that not only the CO_2 concentration in atmosphere is a relevant parameter for membrane-based DAC. Operational parameters such as pressures in the system, number of stages, gas permeance, permeate composition and stage cut (fraction of feed gas that passes through the membrane) influence the energy requirements and must be carefully optimized when aiming for energy efficiency [27]. Furthermore, due to the strict dependence of the membranes' performance on CO_2 concentration, the development of this approach could raise interest and relevance in environments with higher CO_2 concentrations, such as office spaces, where the average CO_2 concentration can reach $1000\ ppm$ [28].

Membrane-based DAC technologies are still in the development stages, i.e., 3–5 TRL. Further research is essential to address the existing challenges and enhance the effectiveness of DAC applications. If current membrane technologies result being unsuitable for DAC applications, the development of new membrane specifically designed for DAC may be necessary. This could introduce significant complexities, which might lead to the complete extinction of interest in this technology.

2.1.4. Electrochemical-based DAC

Electrochemical-based approach could be considered as the direct reduction of CO_2 from the atmosphere as an alternative solution to more conventional DAC technologies [15]. In this method, atmospheric air is supplied at the cathode of an electrochemical cell. Using water, the O_2 present in the air reacts forming hydroxyl groups (OH^-), which can subsequently react with CO_2, capturing it in aqueous solution. Even if this route has been proven to be possible at laboratory scale [29], it is far from optimized, needs further development, and is very unlikely to achieve breakthrough at commercial scale in the next decades.

Apart from the direct electrochemical reduction of CO_2 from the atmosphere, what is more frequently found in literature under the umbrella of electrochemical-based DAC, are the processes that involve the electrochemical regeneration of the sorbent and the release of the captured CO_2. As mentioned, the thermochemical regeneration of the sorbent is the main obstacle that hinders the development of DAC, making this process very energy intensive. Electrochemical-based approaches for the 'unloading' phase can in principle unlock more energy efficient pathways that can make DAC technologies more interesting, while taking advantage of the relatively well-understood and developed electrochemical cells' principles of operation. These types of electrochemical-based DAC are commonly reported as electrochemical carbon capture and concentration (eCCC) and present certain advantages compared to processes based on thermochemical reactions alone. For example, applying a current to directly target redox-active molecules instead of heating or cooling the entire capture medium, may address the limitations of temperature-driven capture and release, while minimizing the heat losses, or facilitating the easier integration with renewable energy sources (RES), as electricity is the only required energy source [30]. It should be noted that eCCC was initially investigated for point-source CO_2 capture, and only recently has their application for DAC attracted significant interest within the scientific community.

eCCC approaches can be broadly divided into three categories: pH-mediated systems, electrochemically mediated amine regeneration (EMAR), and methods involving redox-active capture molecules. The first approach uses electrochemical reactions to vary the pH of an aqueous electrolyte, driving the carbonation reactions and leading in this way to the CO_2 capture or release. An example of this approach consists of the implementation of bipolar membrane electrodialysis (BPMED) for the regeneration of NaOH-based sorbent [31]. EMAR uses amines to capture the CO_2 and an electrochemical cell to drive the CO_2 release and amine regeneration. This method has been primarily developed for the regeneration of amine absorbents used in point-source CO_2 capture, aiming to overcome the limitations associated with the temperature

cycles required for regeneration and the degradation of the amine [32]. The third approach consists of using redox-active capture molecules, which can interact with CO_2 directly binding/releasing CO_2 following changes in oxidation. A generalized redox cycle consists of the reduction of the molecule to form the active state carrier. This reduced species has a high affinity for CO_2 and, upon binding, creates the CO_2-bound adduct, which is finally oxidized, reforming the initial molecule, releasing CO_2, and closing the cycle [33].

The fundamental idea behind each of these methods is the same: to employ well-defined approaches with well-understood chemical and physical principles, with the aim of accelerating the development of carbon capture technologies. While improving the chemistry behind the investigated method and deliver proof-of-concept experiments are important steps, several challenges still limit the potential of electrochemistry-based methods. These include the limited knowledge about large-scale system design and operation, insufficient quantitative data on long-term stability, and the lack of standardized experimental methods and performance metrics. Further research is needed to determine which technologies are best suited to specific boundary conditions. Addressing these gaps will be essential to overcoming current barriers, accelerating implementation, and enabling widespread adoption [30].

2.2. DAC cost

Cost, together with capture technology and energy demand, represents one of the main factors in the deployment of the DAC technologies. Due to the low readiness level of the technology, the calculation of DAC cost proves challenging and remains uncertain. The main figure to consider, to understand if this technology is economically convenient with respect to other carbon capture technologies, is the cost per unit of CO_2 captured, usually expressed as EUR per ton of CO_2 captured $\left(EUR/ton_{CO_2}\right)$. Two of the main factors that contribute to the overall cost of DAC technologies are capital cost and operating cost. The capital cost includes the price for all the equipment pieces that compose the DAC system, while the operating cost includes all the expenses for the operation, maintenance, and labor for the facility [34]. The capital cost is directly related to the capture technology used, while the energy cost, related to the energy demand of the employed technology, frequently contributes the most for the operating costs. Furthermore, the determination of these costs always depends on specific boundary conditions, that differ from case to case, such as the location of the DAC facility and the final use of the CO_2 captured, among the others. Therefore, the identification of one single cost can be ambiguous to be used as benchmark value for these technologies, and for the assessment of techno-economic evaluations [35]. These conclusions are confirmed by data reported by various

companies that have been developing their own DAC technology over the years. Companies such as *Carbon Engineering* (*CE*) [36] have opted to report a range of values rather than a definitive cost for their DAC solutions. This approach is preferred due to the early stage of development of current technology and the numerous factors that come into play, which preclude the definition of a single value. It is often assumed that the lower threshold will be achieved as the technology is scaled up over time. Different companies define the cost of their technology in various ways, considering some factors while neglecting others, depending on what they deem relevant for their own analysis or case study. Therefore, the results found in the literature must always be contextualized and approached with caution, especially when trying to draw conclusions from a direct comparison.

2.3. *Obrist* DAC

To speed up the advancement of DAC, approaches consisting of blending the electrochemical and thermochemical regeneration of the sorbent and release of the captured CO_2 have been researched. This is the case of the DAC technology proposed by *Obrist*. In the proposed system, the absorption step is performed by exploiting a liquid sorbent based on an aqueous solution of NaOH, to capture the CO_2 present in the atmospheric air and produce Na_2CO_3. The following step consists of the electrochemical conversion of Na_2CO_3 to sodium bicarbonate ($NaHCO_3$), through electrolysis.

$$2Na_2CO_3 + 3H_2O \rightarrow 2NaOH + 2NaHCO_3 + H_2 + \frac{1}{2}O_2 \qquad 2.8$$

As shown in global electrolysis reaction (Reaction 2.8), the electrochemical step not only converts Na_2CO_3 into $NaHCO_3$ but also produces H_2 and O_2 at cathode and anode, respectively, and recovers NaOH that is recirculated into the system. Finally, the last step consists of the thermochemical decomposition of $NaHCO_3$, to release the CO_2 captured and recover Na_2CO_3. The system is then completed with two main additional steps that are required to recover and recirculate NaOH and Na_2CO_3. A block flow diagram (BFD) showing the five above-mentioned steps, including the main chemical reactions involved, is proposed in Figure 2.1.

The approach proposed by *Obrist* offers several advantages, particularly for large-scale DAC. Firstly, the adsorption of CO_2 is achieved using NaOH, one of the most widely produced chemical feedstocks globally [37], ensuring no shortage issues for large-scale DAC plants. Secondly, the electrochemical conversion requires only electricity as an input, facilitating integration with RES. Although electrochemical systems that directly regenerate the sorbent and release captured CO_2 have been proposed, they are not yet available for large-scale operation. Consequently, the

Obrist solution, which involves splitting the recovery step into two sub-steps, represents a viable compromise for the rapid development of DAC technology, being both the electrolysis of Na_2CO_3 to $NaHCO_3$ and the thermochemical splitting of $NaHCO_3$, well-established technologies. Furthermore, unlike standard DAC approaches, this method requires only low-temperature heat, enabling easier integration with waste heat recovery solutions or coupling with e-fuel production plants.

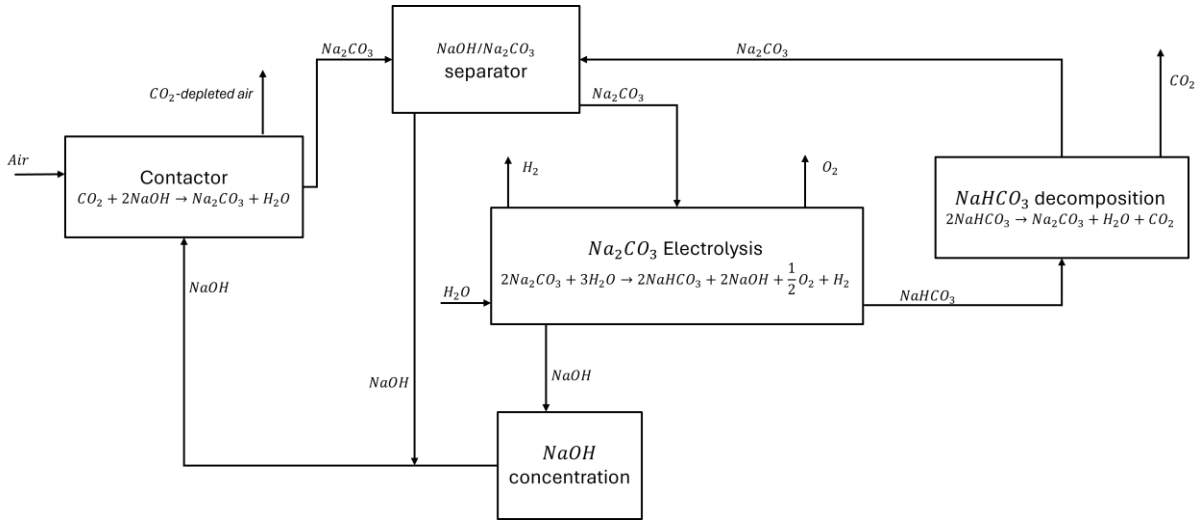

Figure 2.1 Block flow diagram of the system under study

Obrist technology represents a promising approach also from an economic perspective. Given that the various technologies employed in the multiple steps for CO_2 concentration are already well-established, the associated capital costs should be relatively low. Additionally, as technology primarily relies on electrical energy, the operating costs related to energy demand can be minimized by utilizing low-cost RES. Furthermore, the added value of the useful by-products, H_2 and O_2, enhances the relevance of the technology across both DAC and hydrogen production from RES through water electrolysis. This dual benefit makes technology appealing for both DAC and hydrogen generation, enabling its consideration in diverse business cases and scenarios where it can be effectively and economically implemented.

3.Methodology

In this chapter of the report, the methodology followed to carry out the thesis work will be illustrated. A description of the *Aspen Plus* model developed to estimate the energy requirements will be presented, after illustrating the heuristic and assumptions made. Furthermore, the description of the methodology followed to conduct the preliminary economic analysis is discussed.

3.1. Heuristics and assumptions

Various DAC processes have been proposed in recent years. The selection of a specific DAC technology is influenced by numerous factors, with the intended use of the captured CO_2 being particularly significant. As claimed by *Obrist*, the proposed DAC process is highly suitable for coupling with e-fuels production, due to the high purity of the captured CO_2 that can be achieved [10]. For this reason, a scenario in which the captured CO_2 is utilized as input feedstock for CO_2 methanation, to produce synthetic natural gas (SNG) according to the well-known Sabatier reaction (Reaction 3.1), will be considered to carry out the analysis of the system.

$$CO_2 + 4H_2 \rightarrow CH_4 + 2H_2O \qquad 3.1$$

Figure 3.1 presents a schematic of the CO_2 methanation process coupled with DAC and renewable hydrogen production, in which the boundaries of the analysis of this thesis work are highlighted.

DAC processes are usually designed for year-round operation, excluding regular maintenance periods. Assuming a 30-day maintenance period per solar year, an operational year of 8040 hours is considered.

The reliance of electricity from renewable sources is a primary advantage of the DAC process under analysis. However, it is crucial to consider the natural intermittency of RES when planning year-round plant operation. This aspect, while important, falls outside the scope of this analysis and is therefore not considered, with the assumption that a constant electrical energy supply can be guaranteed.

To estimate the normalized energy requirement, expressed in kWh per ton of CO_2 captured $\left(kWh/ton_{CO_2}\right)$, a DAC plant with a nominal CO_2 production supporting a methanation process of $5000\ ton$ of SNG per year $(ton_{SNG}/year)$ is assumed, which results in $1710\ kg$ of CO_2 per

hour. The relative humidity (RH) and temperature of atmospheric air, which vary hourly, highly influence the CO_2 adsorption performance of the air contactor [38].

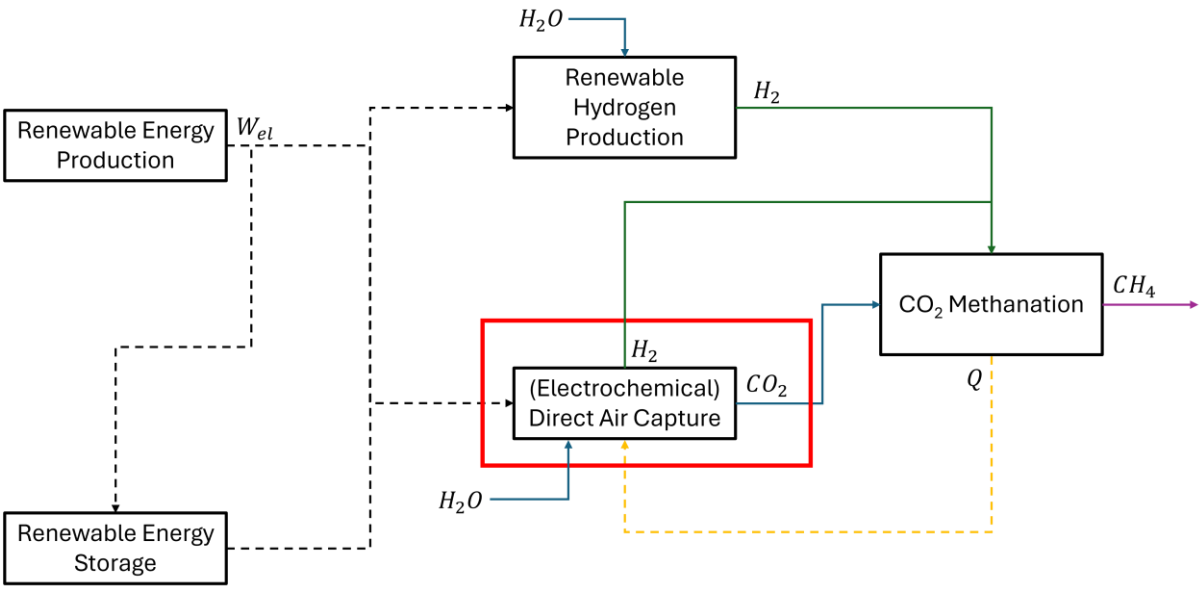

Figure 3.1 Process route for CO_2 methanation combining DAC, RES, and renewable hydrogen. The boundaries of the analysis of this thesis work are delineated by a solid red line

For this analysis, a constant RH of 60% and a constant temperature of 25 °C are assumed for the inlet atmospheric air. The NaOH solution, thanks to its strong binding affinity with CO_2, allows to design the DAC systems with capture rate up to 95%. However, due to several constraints related to the economic and the designing of the air-contactor, the design value typically chosen varies between 50% and 80% [39]. For modeling purposes, fixed capture rate of 75% was assumed. An overview of the inlet air composition and conditions used in the simulation is given in Table 3.1. The atmospheric inlet air has been assumed to be composed of N_2, O_2, CO_2, and water vapor (H_2O). The amount of water vapor has been calculated accounting for the specified RH of 60%, starting from a dry air composition consisting of N_2, O_2 and CO_2 only, where the specified initial concentration of CO_2 on a dry basis was $420\ ppm$.

Table 3.1 Overview of the inlet air feed composition used in the Aspen Plus simulation

	Units	Value
Mass Flow	kg/h	3.81E+06
Molar Flow	$kmol/h$	132030
Mole composition (%)		
N_2		77.528
O_2		20.547
CO_2		0.042
H_2O		1.884
Temperature	°C	25
Pressure	atm	1

3.2. System modeling

The modeling of the system was performed using the *Aspen Plus* software. The electrolyte model ELECNRTL was used, which is intended for electrolyte systems involving partially or completely dissociation of molecular species into ions in liquid solvents and/or precipitation of salts [40]. The following dissociation and precipitation reactions (Reactions 3.2–3.7), considered to be at chemical equilibrium due to their fast reaction rates, were defined as the global chemistry of the simulation:

$$HCO_3^- \leftrightarrow CO_3^{2-} + H^+ \quad (Equilibrium) \qquad 3.2$$

$$H_2O + CO_2 \leftrightarrow HCO_3^- + H^+ \quad (Equilibrium) \qquad 3.3$$

$$H_2O \leftrightarrow OH^- + H^+ \quad (Equilibrium) \qquad 3.4$$

$$NaOH \rightarrow OH^- + Na^+ \quad (Dissociation) \qquad 3.5$$

$$Na_2CO_3 \rightarrow CO_3^{2-} + 2Na^+ \quad (Dissociation) \qquad 3.6$$

$$NaHCO_3 \rightarrow HCO_3^- + Na^+ \quad (Dissociation) \qquad 3.7$$

All the required parameters, physical and chemical properties of the components involved in the process, which were defined in the compounds list of the simulation, were retrieved directly from the *Aspen Plus* database. In this initial attempt to model the system, with the aim of estimating the specific energy consumption of the process, the complete dissociation of the involved salts in aqueous solution was assumed, neglecting the possible formation of precipitation. However, this was taken into account by ensuring that the different solutions involved always remained below the solubility limits. As presented in the BFD of the system (Figure 2.1), the overall system can be divided into five different subsystems: the air-contactor

subsystem, the Na_2CO_3 electrolysis subsystem, the $NaHCO_3$ thermochemical decomposition subsystem, the NaOH concentration subsystem, and the NaOH/Na_2CO_3 separation subsystem. Each of these subsystems were first modeled separately and then integrated together. The total resulting energy consumption of the process was therefore described by the summation of the energy consumption in each of these five subsystems.

An overview of the process flow diagram (PFD) of the modeled system is presented in Figure 3.2. The PFD, in which the five subsystems are highlighted, is provided in Appendix A. Ambient air is fed to the air-contactor unit, where it is contacted with an aqueous solution of NaOH. The CO_2-rich capture solution is feed into the electrochemical cell, in which the carbonate is converted into bicarbonate and the solvent is regenerated. In the final step, the bicarbonate is thermochemically decomposed, releasing the captured CO_2 and the carbonate, which is recirculated into the system. A more in-depth description of each of these subsystems will be provided in the following sections in the chapter.

3.2.1. Air-contactor subsystem

In the air-contactor subsystem, the inlet atmospheric air is brought into contact with the aqueous solution of NaOH, with the aim of absorbing CO_2 to produce Na_2CO_3, according to the global exothermic reaction 3.8, and releasing the CO_2-depleted air into the external environment.

$$CO_2 + 2NaOH \rightarrow Na_2CO_3 + H_2O \; \Delta H = -109.4 \; kJ/mol \qquad 3.8$$

The process begins with the physical dissolution of CO_2 into the liquid phase. Successively, the dissolved CO_2 reacts with the OH^- ions present in the solution due to the dissociation of NaOH, forming bicarbonate ions (HCO_3^-). Finally, HCO_3^- reacts with an additional OH^-, producing bicarbonate ions (CO_3^{2-}) and H_2O. These steps can be summarized by the following reactions (Reactions 3.9–3.12).

$$CO_{2\,(g)} \leftrightarrow CO_{2\,(l)} \qquad 3.9$$

$$NaOH \leftrightarrow Na^+ + OH^- \qquad 3.10$$

$$CO_2 + OH^- \leftrightarrow HCO_3^- \qquad 3.11$$

$$HCO_3^- + OH^- \leftrightarrow CO_3^{2-} + H_2O \qquad 3.12$$

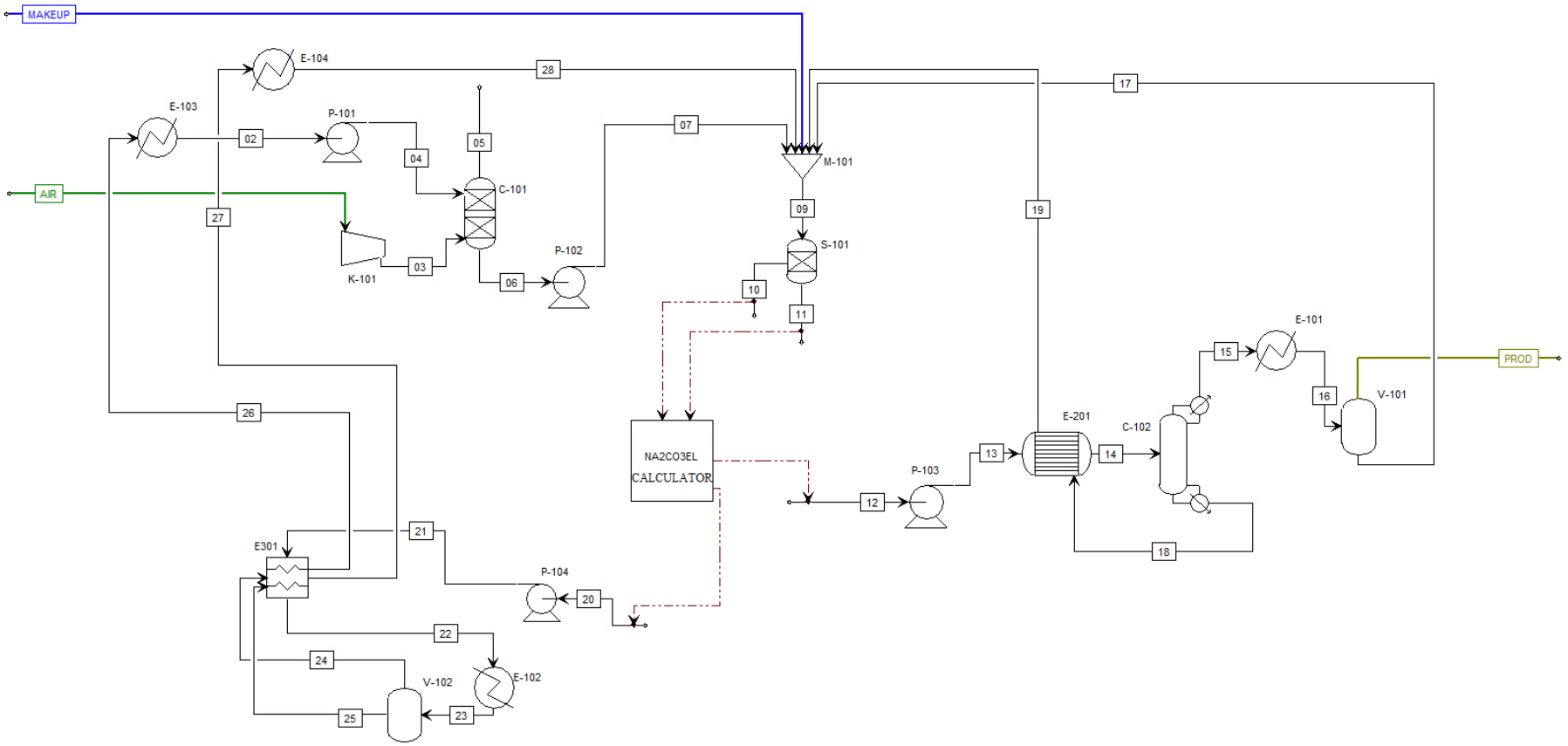

Figure 3.2 Process flow diagram of the Aspen Plus developed model

Reaction 3.12 describes the proton transfer reaction, which is considered instantaneous and reversible, with a much higher rate constant than Reaction 3.11, which therefore governs the overall rate of reaction [41]. Initially, due to the high concentration of OH^-, the absorption process is dominated by the formation of carbonate ions.

As the reaction proceeds, the high consumption of OH^- results in a decrease in pH and when values around 10.25 are reached, the formation shifts towards bicarbonate ions. Therefore, the formation of carbonate ions is enhanced by maintaining a high value of pH, using a concentrated NaOH solution (greater than $1\ mol/L$) and optimizing the absorption condition, including the design of the air-contactor to increase the specific surface area for gas-liquid interaction [42]. As previously mentioned, the aim of the air-contactor subsystem is to produce Na_2CO_3, which is considered a first intermediate product, sent to the electrochemical cell to produce $NaHCO_3$, which is then thermochemically decomposed to release the captured CO_2. The electrochemical cell not only produces $NaHCO_3$ but also regenerates NaOH, allowing the system to operate in a closed loop. It is therefore of utmost importance to optimize the contactor towards the formation of carbonate, as the formation of bicarbonate results in a loss of solvent that must be replenished from external sources.

For evaluating the energy consumption, the air-contactor was modeled with an absorption column, where the reaction between CO_2 and NaOH occurs; a compressor, which represents the fan that drives the inlet air toward the contactor; and a pump, used to ensure the recirculation of the liquid sorbent. As the electrical work required to operate the pump is orders of magnitude lower than the electrical power required by the compressor, the energy consumption related to the air-contactor is associated to the energy required by the compressor only. The absorber is modeled using the RADFRAC model. This model was selected because it enables more rigorous calculation than other distillation models in *Aspen Plus*.

3.2.2. Na_2CO_3 electrolysis subsystem

As described by the global electrochemical reaction presented in Section 2.3, the electrochemical cell is used to convert Na_2CO_3 into $NaHCO_3$, regenerate NaOH, and produce useful by-products (H_2 and O_2). The global reaction (Reaction 2.8) can be interpretated as the combination of the oxygen evolution reaction (OER) occurring at the anode (Reaction 3.13), where Na_2CO_3 is converted into $NaHCO_3$ and O_2 is released, and the hydrogen evolution reaction (HER) occurring at the cathode (Reaction 3.14), where NaOH is regenerated by means of sodium ions (Na^+) coming from the anode side through a cation exchange membrane, and H_2 is released.

$$2Na_2CO_3 + H_2O \rightarrow 2NaHCO_3 + 2Na^+ + \frac{1}{2}O_2 + 2e^- \quad Anode\ (OER) \qquad 3.13$$

$$2H_2O + 2Na^+ + 2e^- \rightarrow 2NaOH + H_2 \quad Cathode\ (HER) \qquad 3.14$$

Due to the lack of a specific model for electrochemical devices in *Aspen Plus*, the electrochemical cell was simulated using a calculator block wherein the behavior of the cell is considered by implementing all the governing equations utilizing an *Excel* spreadsheet linked to it. This approach aims to ensure the overall mass balance of the system and estimate the energy consumption of the electrochemical device. The implemented equations are based on the experimental work published by Liu et al. [43]. In their work, the electrolysis of Na_2CO_3 is interpreted as the electrolysis of H_2O followed by the protonation of CO_3^{2-} to HCO_3^-. The voltage required to drive the reaction is higher than the voltage required for the electrolysis of water, due to the transport of Na^+ through the cation exchange membrane, which increases the ohmic overvoltage, and the presence of other ions in the anolyte and catholyte sections, which contributes to the increase in concentration overvoltage.

To evaluate the energy consumption of the electrochemical cell, the total current required to produce the amount of H_2 proportional to the desired amount of $NaHCO_3$ is first evaluated, considering that two moles of electrons (e^-) are required to produce one mole of H_2. Subsequently, considering the experimental average voltage measured at a given value of current density by Liu et al., and the associated Faradaic efficiency, which accounts for all sources of loss in the system, the total power required by the system is obtained. Finally, considering the total operating time of the system and the amount of CO_2 produced, the specific energy consumption is determined. At this stage of the work, other additional components supporting the operation of the electrochemical cell are not considered, and the energy consumption associated with it is exclusively intended as the electrical energy required to run the electrochemical cell only.

3.2.3. $NaHCO_3$ thermochemical decomposition subsystem

The thermochemical decomposition of $NaHCO_3$ is the final step of the process, in which $NaHCO_3$ is thermochemically decomposed, to release the captured CO_2 and recover Na_2CO_3 (Reaction 3.15).

$$2NaHCO_3 \rightarrow Na_2CO_3 + H_2O + CO_2 \qquad 3.15$$

The decomposition of $NaHCO_3$, which starts already at temperature of 50 °C and does not require any catalyst to proceed, was modeled in *Aspen Plus* by means of another RADFRAC column, equipped with a reboiler that provides the required heat to carry out the reaction, and condenser that allows the separation between the liquid and vapor phases. The column is supported by a heat exchanger, used to recover heat from the material stream exiting the bottom of the column to preheat the inlet stream, and a condenser and gas-liquid separator to effectively separate the vapor water and the CO_2 produced. To more efficiently perform the reaction inside the distillation column and to contrast pressure drops in the column and heat exchangers, the flow rate of $NaHCO_3$ solution exiting from the anode of the electrochemical cell is first pressurized by means of a pump to an adequate level of pressure. However, when evaluating the energy consumption of the subsystem, the electrical energy required to run the pump is considered negligible compared to the thermal energy required to perform the thermochemical decomposition of $NaHCO_3$, which is therefore considered the only input energy required for this subsystem.

3.2.4. NaOH concentration subsystem

An important aspect of all the DAC technologies concerns the regeneration of the sorbent medium used to capture the CO_2 from the atmospheric air. If the process was not able to regenerate the sorbent, which would need to be continuously replenished from external sources, it would never be considered sustainable from an economic perspective. In the system proposed by *Obrist*, the liquid sorbent NaOH is regenerated in the electrochemical cell and then recirculated into the air-contactor, ensuring the possibility to operate in a closed loop. However, due to different concentrations of NaOH in the catholyte section of the electrochemical cell, and the resulting different concentration of the produced NaOH solution compared to the concentration required at the air-contactor for effective CO_2 absorption, the NaOH solution needs to be concentrated. The concentration of the NaOH solution is performed thermally, by means of water evaporation. As for the anode side, the NaOH solution exiting from the cathode is first pressurized, to effectively contrast the pressure losses in the downstream components. and then sent to a heat exchanger where the desired amount of water is evaporated first and separated afterward into a gas-liquid separator. The subsystem is completed with another heat exchanger for heat recovery and additional coolers to regenerate the temperatures of the recirculated streams. In this case as well, the electric energy required to operate the pump is negligible compared to the thermal energy required to evaporate water and thus is neglected. The energy consumption of the subsystem is associated solely with the required thermal energy.

3.2.5. NaOH/Na_2CO_3 separation subsystem

The final subsystem required to complete the system consists of a separator between NaOH and Na_2CO_3. The outlet stream of the air-contactor, consisting of unreacted NaOH, H_2O and Na_2CO_3, and the recirculated stream from the bottom of the distillation column of the $NaHCO_3$ thermochemical decomposition subsystem are brought into contact, with the aim of separating Na_2CO_3 from NaOH before sending it to the anode of the electrochemical cell and recirculating the unreacted NaOH. In *Aspen Plus*, there is no specific block that allows for proper modeling of this separation; therefore, this part of the process was simulated using a mixer and a separator, where the desired separation of components is imposed. The energy consumption of this subsystem is evaluated by referencing information available in the literature about specific technologies that can facilitate this separation.

3.2.6. Water balance

As already presented, the main reactions that drive the overall DAC process are three: the CO_2 absorption reaction at the air-contactor (Reaction 3.8), the Na_2CO_3 electrolysis reaction at the electrochemical cell (Reaction 2.8), and the $NaHCO_3$ thermochemical decomposition reaction at the $NaHCO_3$ thermochemical decomposition column (Reaction 3.15). These reactions have already been well summarized in the BFD of the process proposed in Figure 2.1. As can be seen from the stoichiometry of the aforementioned reactions, three moles of H_2O are required to produce one mole of CO_2, two of which are internally produced by the system, at the air-contactor and at the $NaHCO_3$ thermal decomposition column, respectively, and one must be continuously provided from external sources to the system, corresponding to the mole of H_2O that undergoes the water electrolysis reaction and produces H_2 and O_2. However, due to two main sources of water losses in the process, occurring at the air-contactor, with the CO_2-depleted air leaving the system, and at the $NaHCO_3$ decomposition subsystem, with the released CO_2, which is not completely dry, additional makeup water must be supplied. This makeup water is supplied at the subsystem that models the NaOH/Na_2CO_3 separation, together with the recirculated water from the NaOH concentration subsystem and the $NaHCO_3$ thermochemical decomposition subsystem.

3.3. System sizing

The next step after completing the *Aspen Plus* model involves performing the sizing of the different equipment that composes the system, in order to estimate the main design specifications. The sizing of the more conventional process equipment, such as heat exchangers,

pumps, and the column for the $NaHCO_3$ decomposition, has been performed directly in *Aspen Plus*. The vertical vessels used for gas-liquid separation are sized using the *Vessel Design Tool*, an internal software developed by *Shell*, which ensures compliance with the most up-to-date rules for the sizing of these components. Special attention is given to the sizing of the air-contactor and the electrochemical cell. The modeling of the air-contactor using a compressor for the inlet atmospheric air and an adsorption column for the reaction between the CO_2 and the liquid sorbent represents a reliable way to estimate the energy consumption of the subsystem. However, it does accurately represent the real behavior of the system, as specific designs are required to maximize the specific contact area between the liquid and the gas and minimize pressure drops. Therefore, the sizing and design of this component are carried out considering the information reported in the literature for already well-developed air-contactor solutions for DAC applications proposed by other researchers. The same reasoning is applied to the sizing of the electrochemical cell. Since this component is not directly simulated by a built-in model in *Aspen Plus*, its sizing is carried out using experimental results found in the literature.

3.4. Preliminary economic analysis

A cost analysis is usually performed in the early development stage of a project in order to assess and compare its economic feasibility with alternative processes. The aim of the preliminary economic analysis described here is to evaluate the overall cost of the CO_2 capture process under study and compare it with other alternative processes present in the literature. The final result, which will be presented as currency per ton of captured CO_2, is achieved by evaluating the capital expenditures and the operational expenditures associated with the process. Furthermore, additional considerations will be undertaken to evaluate the economic benefits associated with the valuable by-products generated alongside the captured CO_2. Additionally, for the quantities for which the evaluation of the associated cost is intrinsically uncertain, due to the lack of information or the difficulties encountered in effectively predicting the cost, a sensitivity analysis will be carried out to evaluate how variations in these quantities impact the final cost.

3.4.1. Capital expenditures

The capital expenditure (CAPEX) represents the fixed assets of a company, such as equipment, building and property. The evaluation of the cost associated with the more conventional process equipment (heat exchangers, pumps, gas-liquid separation vessels) is performed using the *Aspen Process Economic Analyzer* (APEA) tool, which relies on an up-to-date database of information that allows for realistic estimation of the capital expenditure associated with these components. The capital cost of the air-contactor, which represents the component that deviates the most

from more traditional process equipment in terms of sizing and design, is estimated by following the air-contactor cost optimization model proposed by Keith et al. [44]. Finally, the capital cost of the electrochemical cell is estimated based on the most up-to-date information available in the literature for this type of electrochemical device.

3.4.2. Operational expenditures

Operational expenditures (OPEX) represent ongoing expenses necessary for the day-to-day functioning of the business, such as raw materials, utilities, maintenance, operating labor, license fees, and plant overheads. In this preliminary economic analysis, the focus will primarily be on the cost of the utilities that are needed to run the process. Specifically, the cost of the thermal energy, electricity, and makeup water required to operate the DAC plant are quantified and discussed. Additionally, the cost associated with the utilities required for the main balance of plant (BoP) components, such as the cooling water required at the heat exchangers, will also be considered.

3.4.3. Capture cost

After estimating the CAPEX and OPEX of the system, the capture cost of the process is evaluated according to the following definition (Equation 3.16) [45]:

$$Capture\ cost = \frac{TOC \cdot CCF + C_{O\&M}^{fix} + C_{O\&M}^{var} \cdot h_{eq}}{F_{CO_2} \cdot h_{eq}} \qquad 3.16$$

In this equation, TOC refers to the total overnight capital, defined in accordance with NETL guidelines [46], [47]. The capital charge factor (CCF) accounts for cost escalation and interest incurred during the construction phase, and it depends on the financial methodology adopted for the project as well as various other financial parameters. The fixed and variable operation and maintenance costs, denoted as $C_{O\&M}^{fix}$ and $C_{O\&M}^{var}$, include expenses related to maintenance, labor, insurance and utilities. The term F_{CO_2} represents the mass flowrate of captured CO_2, while h_{eq} denotes the equivalent annual operating hours, which account for plant availability and are defined as the ratio of actual operating hours to the total number of hours in a year.

4.Results and discussion

In this chapter, the main findings from the analysis of the studied process will be presented and discussed. First, an overview of the primary results obtained from the *Aspen Plus* model, that was developed to simulate the DAC process, will be provided. Subsequently, based on these results and on the additional results obtained from the modeling procedures developed to estimate the specific energy consumption of the subsystems not directly modeled in *Aspen Plus*, the evaluation of the specific energy consumption of the process will be presented. The second part will explain the results related to the sizing of all major components of the process, along with the corresponding outcomes derived from the economic analysis. Finally, concluding remarks and considerations regarding the studied process, in comparison with alternative processes available in the literature, will be presented.

4.1. System modeling results

The process model has been developed considering to produce the amount of CO_2 required to support a CO_2 methanation process with a SNG production capacity of 5000 tons per year. The resulting quantity of captured CO_2 is 14.2 kilotons per year. Additionally, the overall process yields $621\ ton$ of H_2 per year as by-product. The amount of treated air required reported in Table 3.1 is higher than the stoichiometric requirement, mainly due to the air-contactor's fixed CO_2 capture rate of 75%.

The PFD of the developed *Aspen Plus* model has been presented in Figure 3.2. The details regarding the streams of the process are reported in Appendix B. The overall process can be divided into five distinct subsystems. The first main subsystem, the air-contactor subsystem, involves bringing atmospheric air into contact with an aqueous NaOH solution to capture CO_2 and produce Na_2CO_3, as described by Reaction 3.8. Due to the strong affinity of NaOH for CO_2, a relatively low hydroxide concentration ($1\ mol/L$) is sufficient to drive the reaction in the desired direction, achieving a capture efficiency of up to 95%. However, as the pH decreases due to the reduction in OH^- concentration, the formation of HCO_3^- is favored over CO_3^{2-}. To maintain a pH above 10.25 and ensure the predominance of carbonate formation, a higher NaOH concentration is required. Therefore, a $6\ mol/L$ NaOH solution has been selected for the inlet lean sorbent, resulting in a pH of approximately 13.5. This concentration also helps minimizing water losses associated with the CO_2-depleted air exiting the contactor [7], [48]. This subsystem has been modeled using a compressor to estimate the electrical energy required for the forced convection of atmospheric air into the contractor, and an adsorption column to simulate the

reaction between air and the adsorption solvent, as well as the gas-liquid phase separation. It is important to emphasize, however, that while this modeling approach provides a reasonable estimate of energy requirements, the actual configuration of the air-contactor differs significantly from a conventional vertical adsorption column typically used in the chemical industry. This is primarily due to the low CO_2 concentration in the inlet air stream, which necessitates a large contact area between the liquid and gas phases and substantial pumping energy for the liquid sorbent. For these reasons, the design and sizing of the air-contactor have been carried out using the optimized methodology developed by Keith et al. [44], which will be discussed in Section 4.2.

The second main subsystem models the electrolysis of Na_2CO_3, which serves to regenerate NaOH and convert Na_2CO_3 into $NaHCO_3$, while also producing H_2 and O_2 as by-products of the water electrolysis reaction. This subsystem is implemented using a calculator block, in which a spreadsheet is employed to model the mass balance equations necessary for continuous operation, as well as the chemical reactions occurring at the electrodes, with the aim of estimating the energy consumption of the electrochemical device, starting from the experimental results published by Liu et al. [43]. The electrochemical cell is set to operate at 40 °C and $1\ atm$, same operating conditions used by Liu et al. The electrochemical reactions at the cathode and anode have already been introduced in Section 3.2.2 (Reactions 3.13, 3.14). The total energy consumption of the electrolysis subsystem is associated with the energy required for the electrochemical cell only and is evaluated as follows (Equation 4.1):

$$E = V \cdot I \cdot t \qquad 4.1$$

where V is the operating voltage of the cell, assumed to be equal to the average value $2.63\ V$, according to the experimental results reported by Liu et al., obtained at current density of $120\ mA/cm^2$. I represents the total current required, which is proportional to the amount of H_2 produced, and is calculated using the well-known Faraday's law (Equation 4.2), incorporating a Faradaic efficiency of 0.918 as reported by Liu et al. t represents the operating time of the cell.

$$I = \frac{n \cdot \dot{n}_{H_2} \cdot F}{\eta_{Faradaic}} \qquad 4.2$$

In Equation 4.2, n is the numbers of electrons transferred per mole of hydrogen produced (equal to 2), $\dot{n}_{H_2}$ represents the molar flow rate of H_2, $F = 96485 C/mol$ is Faraday's constant, and $\eta_{Faradaic}$ is the Faradaic efficiency. Based on the amount of H_2 produced, the total current required is calculated to be $2263460\ A$.

The final main subsystem models the thermochemical decomposition of $NaHCO_3$, as described by Reaction 3.15. The $NaHCO_3$ produced at the anode of the electrochemical cell is directed to a distillation column equipped with a reboiler, which supplies the necessary thermal energy via medium-pressure steam, and a partial condenser, which facilitates the effective separation of gaseous and liquid products. Prior to entering the column, the stream is pressurized to 3 bar, to compensate for pressure losses in the heat exchanger, used for process-to-process heat integration, and within the column itself. A pressure drops ranging from 0.3 to $0.5\ bar$ is imposed across all heat exchanger and coolers used throughout the process. Although the thermochemical decomposition of $NaHCO_3$ starts already at 50 °C, the column is operated at a design temperature of 140 °C, to ensure a sufficiently high reaction rate. The resulting gaseous products are subsequently cooled using cooling water at 25 °C to a final temperature of 40 °C. The released CO_2 is then separated from the condensed water in a gas-liquid separator vessel. Both the recovered water and the regenerated Na_2CO_3 are recirculated into the system to close the material loop.

The aqueous NaOH solution is assumed to be produced at the cathode of the electrochemical cell with a resulting concentration of $3\ mol/L$, as reported by Liu et al. Consequently, this concentration must be increased to reach the target design concentration required at the inlet of the air-contactor. This concentration step, carried out in the previously called NaOH concentration subsystem, is achieved by providing thermal energy via medium-pressure steam, following process-to-process heat integration, to evaporate the necessary amount of water, which is subsequently condensed and recirculated within the system. As in the $NaHCO_3$ decomposition subsystem, the inlet stream is first pressurized to $3\ bar$ to compensate for pressure drops across the heat exchangers and the gas-liquid separator vessel. Both the regenerated solvent and the recirculated water are cooled down to 40 °C using cooling water at 25 °C. It was obtained that maintaining the lean solvent at a temperature slightly above ambient does not negatively affect the adsorption performance of the air-contactor. Therefore, further cooling has been avoided, eliminating therefore the need for chilled water.

Lastly, prior to introducing the produced and recirculated Na_2CO_3 into the electrochemical cell, a separation step is theoretically required to remove excess unreached NaOH. The presence of excess NaOH is in principle required for maintaining the desired level of alkalinity within the air contactor. However, the separation of Na_2CO_3 from NaOH in aqueous solution presents significant challenges, as it is not straightforward, and no established methods or technical evidence are currently available in the literature to facilitate this process. One potential approach to achieve this separation involves manipulating the pH of the mixture to reduce the

solubility of Na_2CO_3 in the NaOH solution, inducing its precipitation. The resulting solid phase could then be separated from the liquid phase and subsequently washed to regenerate an aqueous Na_2CO_3 solution suitable for introduction into the anode compartment of the electrochemical cell. However, in this first attempt to model the process, it was decided to not account for the formation of solid phases, ensuring that all aqueous streams within the process remain below their respective solubility limits. Therefore, also due to the resulting relatively low concentration of NaOH at the outlet of the air-contactor subsystem, the NaOH/Na_2CO_3 separation subsystem has been omitted from the system configuration, excluding it, therefore, also for the evaluation of the specific energy consumption of the process. Instead, the produced and recirculated Na_2CO_3 is directly introduced into the electrochemical cell after its concentration is adjusted with an appropriate amount of water. This adjustment primarily compensates for the water losses occurring in the air-contactor. For the purposes of the simulation, a single water makeup stream is considered. However, it is important to note that a portion of this water is directed to the cathode compartment of the electrochemical cell to supply the necessary reactant for the water electrolysis reaction.

4.1.1. Process specific energy consumption

An overview of the specific energy consumption associated with the process, normalized per ton of CO_2 produced and disaggregated by subsystems, is presented in Figure 4.1. The total specific energy consumption of the process amounts to approximately $1200\ kWh$ per ton of CO_2 in electrical energy and $1400\ kWh$ per ton of CO_2 in low-temperature thermal energy. As previously discussed, the process relies on two primary energy sources: electricity and low-temperature heat. Electricity is assumed to be supplied by low-cost RES, while thermal energy is provided in the form of medium-pressure steam. This steam is assumed to be sourced from the boiler feedwater utility, which recovers waste heat from the CO_2 methanation process. To highlight the distinct nature and energy quality of these two forms of energy, the specific energy consumption is reported on two separate axes, one for the electrical energy and one for the low-temperature thermal energy. It is important to emphasize that the reported energy consumption accounts exclusively for the operation of the DAC process. Specifically, for the air-contactor, NaOH concentration, and $NaHCO_3$ thermochemical decomposition subsystems, the reported values represent the actual energy required for their operation. However, for the Na_2CO_3 electrolysis subsystem, the reported energy does not include the energy required for the water electrolysis reaction that leads to the production of H_2. As a consequence, the actual energy demand for operating the electrochemical cell is higher than the reported value.

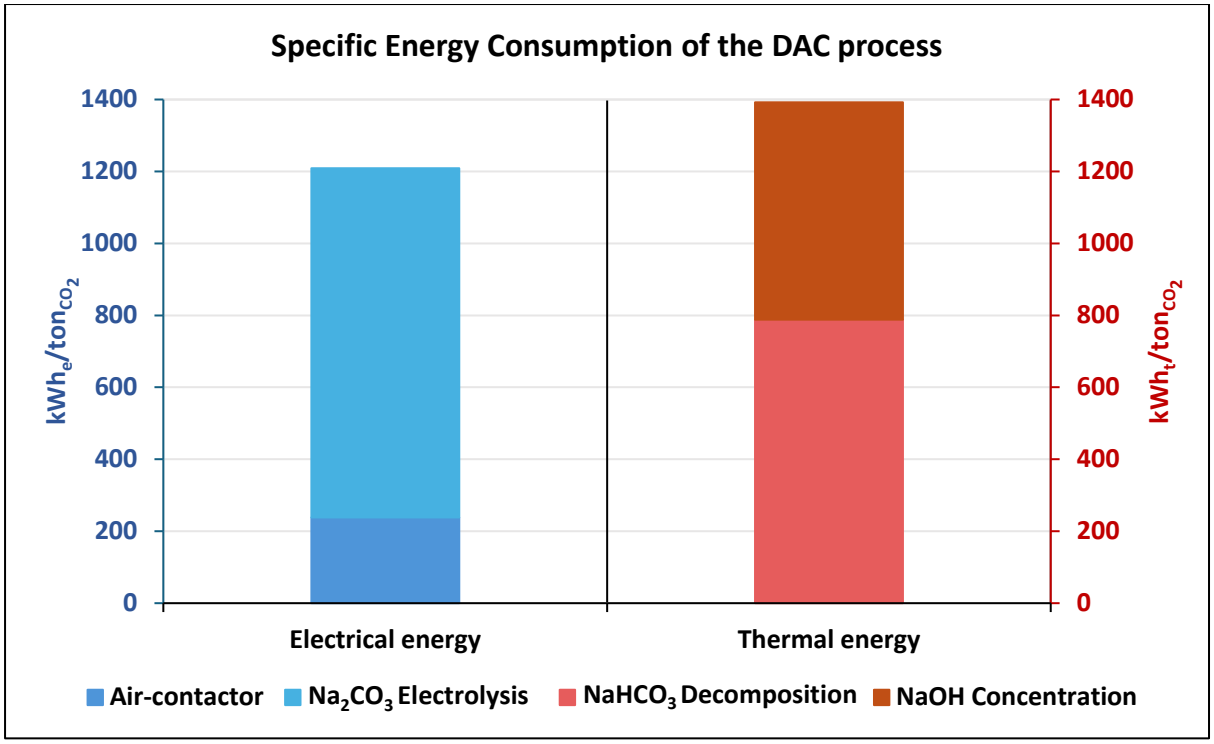

Figure 4.1 Specific energy consumption of the DAC process

The energy consumption associated with the Na_2CO_3 electrolysis subsystem was initially evaluated based on experimental data reported by Liu et al. [43], resulting in a value of $3489.5\ kWh_e/ton_{CO_2}$. This value represents the total energy required to operate the electrochemical cell, including both the production of $NaHCO_3$ and the generation of H_2 as a by-product. However, since the focus of this analysis is on the energy demand of the DAC process alone, it was necessary to isolate the portion of energy consumption attributable to the DAC function only. To achieve this, the energy required to produce an equivalent amount of H_2, matching the quantity generated as a by-product of Na_2CO_3 electrolysis, was estimated using an efficiency of $55\ kWh$ per kilogram of H_2 produced, which is typical for a state-of-the-art alkaline water electrolyzer [49]. This value, normalized per ton of CO_2 captured and resulting in $2519.5\ kWh_e/ton_{CO_2}$, was then subtracted from the total energy consumption derived from the experimental data. The resulting difference represents the net energy required to operate the electrochemical cell exclusively for the DAC process, i.e., for the conversion of Na_2CO_3 to $NaHCO_3$ and the subsequent release of captured CO_2. This adjusted value is the one reported in Figure 4.1, as it more accurately reflects the energy demand of the DAC process. However, it is crucial to note that this energy value alone is not sufficient to fully operate the electrochemical cell, as it does not account for the energy required to carry out the water electrolysis reaction.

4.1.2. Water losses

The makeup water supplied to the $NaOH/Na_2CO_3$ subsystem is required to compensate for water losses occurring in two main subsystems: the air-contactor and the $NaHCO_3$ thermochemical decomposition subsystem. In the air-contactor, water is lost with the CO_2-depleted air exiting the system, while in the $NaHCO_3$ thermochemical decomposition subsystem, water is lost due to the incomplete drying of the produced CO_2 stream. In addition to these losses, one additional mole of water per mole of CO_2 captured is required as a reactant for the water electrolysis reaction. However, since this water is converted into H_2, which is considered as a valuable by-product of the process, it is not considered a net loss. Taking into account the water losses from both the air-contactor and the CO_2 stream, the required external water supply was calculated to be 5.7 tons of water per ton of CO_2 captured. It is important to note that this value corresponds to water losses under specific atmospheric inlet conditions. Water losses are highly sensitive to environmental parameters, particularly to RH and are primarily influenced by the operating and design condition of the air-contactor. Generally speaking, lower RH values result in higher water losses due to the increased water uptake capacity of drier atmospheric air. Conversely, at higher RH levels, the air has a reduced capacity to absorb additional moisture, thereby decreasing water losses. As a result, since DAC systems in real-world conditions operate under varying RH levels, the literature typically reports a range of water loss values rather than a single fixed figure. The value obtained in this analysis is consistent with the value reported in the literature for other DAC processes $\left(4 - 9\ ton_{H_2O}/ton_{CO_2}\right)$ [50].

4.2. System sizing results

A list of the equipment used to model the process in *Aspen Plus*, corresponding to the PFD presented in Figure 3.2, is provided in Table 4.1. As previously mentioned, conventional equipment such as pumps, heat exchangers, and the distillation column employed for the thermochemical decomposition of $NaHCO_3$ were sized directly within *Aspen Plus*. Gas-liquid separator vessels were dimensioned using the *Vessel Design Tool* developed by *Shell*. The equipment used to simulate the air-contactor subsystem was not employed for direct sizing purposes, as the design of this subsystem deviated significantly from conventional chemical process equipment. Detailed information regarding the sizing methodology for this subsystem is provided in Section 4.2.1, along with the sizing approach for the electrochemical cell (Section 4.2.2), which, as previously discussed, is not directly modeled in *Aspen Plus*. Additionally, components intended to close the material loop, with the $NaOH/Na_2CO_3$ separation subsystem, although reported in the equipment list, were excluded from the system sizing, and the

subsequent economic analysis, as this subsystem was ultimately not considered in the process design.

Table 4.1 Equipment list

No.	Equipment	No.	Equipment	No.	Equipment
K-101	Compressor	**C-101**	Absorption column	**E-104**	Cooler
P-101	Pump	**C-102**	Decomposition column	**E-201**	Heat Exchanger
P-102	Pump	**E-101**	Cooler	**E-301**	Heat Exchanger
P-103	Pump	**E-102**	Cooler	**V-101**	Vessel
P-104	Pump	**E-103**	Cooler	**V-102**	Vessel
M-101	Mixer	**S-101**	Separator		

The heat exchangers used throughout the process, including the reboiler required to supply heat to the decomposition column (not explicitly shown in the PFD), were sized assuming conventional shell-and-tube configurations. Stainless steel was selected as the construction material for all heat exchangers, vessels and the decomposition column. A detailed overview of the equipment specifications, such as heat duty and equipment sizes, can be found in Appendix C.

4.2.1. Air-contactor sizing

The air-contactor is the subsystem responsible for capturing CO_2 directly from atmospheric air and represents one of the core components of any DAC system. This unit differs significantly from conventional adsorption typically used in the chemical industry, primarily due to the low concentration of CO_2 in ambient air and the correspondingly high volumetric flow rates required to capture meaningful quantities of CO_2. These unique operational constraints necessitate the development of highly efficient air-contactor designs, particularly to minimize the associated energy consumption.

Over the years, various design solutions have been proposed, and research continues to optimize these systems in terms of both energy efficiency and cost. For the purposes of this thesis work, the design of the air-contactor is based on the optimization model developed by *Carbon Engineering* (*CE*), a company that has been actively working on the design and optimization of liquid-sorbent-based air-contactors since 2009. The key results of their work, as reported in the literature, are used here to estimate the size of the air-contactor required for the system under study.

The adopted design features a crossflow slab geometry, in which air flows orthogonally to the gravity-driven downward flow of the liquid sorbent. The contactor is relatively thin along the air flow axis compared to its height and length. Structurally, the air contactor can be divided into

two main components: the shell and the packing. The shell includes an external framework, fans for inducing forced air convection, and pumps for distributing the liquid sorbent. The packing, contained within the shell, provides the surface area necessary for gas-liquid contact and includes specialized supports and fluid distribution systems. The packing material, which constitutes the core of the air-contactor, is made of plastic. This material was selected based on its ability to meet several critical criteria: (1) chemical resistance to the hydroxide solution used for CO_2 absorption, (2) long service life, (3) low air-side pressure drops, (4) effective CO_2 uptake performance, (5) low cost, and (6) resistance to fouling [51].

The energy required to operate the air-contactor consist primarily of the power needed to drive the air fans, and to a lesser extent, the liquid pumps. The energy demand associated with the liquid pumping is considered negligible. This is due to the low liquid-to-gas ratio employed, which allows for intermittent wetting of the packing material and significantly reduces pumping requirements. Consequently, fan power becomes the dominant factor influencing the system's energy consumption and design. Energy consumption of the fan is influenced by the operating air velocity and the depth of the packing. Higher air velocities increase fan power requirements, while lower velocities require greater packing depth to maintain the same CO_2 capture rate per unit of contactor volume. According to the optimization model proposed by Keith et al. [44], the resulting optimal air velocity and packing depth are $1.5\ m/s$ and $5.5\ m$, respectively. The corresponding pressure drops across the packing, calculated using the same model, is $91\ Pa$. To estimate the fan power using the compressor model in *Aspen Plus*, a pressure increase of $400\ Pa$ was assumed, yielding to a fan power requirement consistent with the values that can be obtained by the optimization model.

It is important to note that the proposed optimization model was developed primarily to minimize the overall cost of the air-contactor system. For this reason, the sizing results are closely related to economic considerations, which will be discussed in detail in Section 4.3.1 of the economic analysis. Based on this model, the air-contactor unit designed by *CE* is capable of capturing 100 kilotons of CO_2 per year, with overall dimensions of $7\ x\ 20\ x\ 200$ meters and an inlet frontal area of $4000\ m^2$. This unit then can be assumed to be composed of modular sub-units, each measuring $5\ x\ 5$ meters in frontal area. The use of standardized sub-units can enable shop fabrication and field assembly, thereby reducing labor costs and eliminating the need for on-site construction. To facilitate a clearer understanding of the air-contactor geometry, a conceptual design is presented in Figure 4.2, where the modular sub-units are also identifiable.

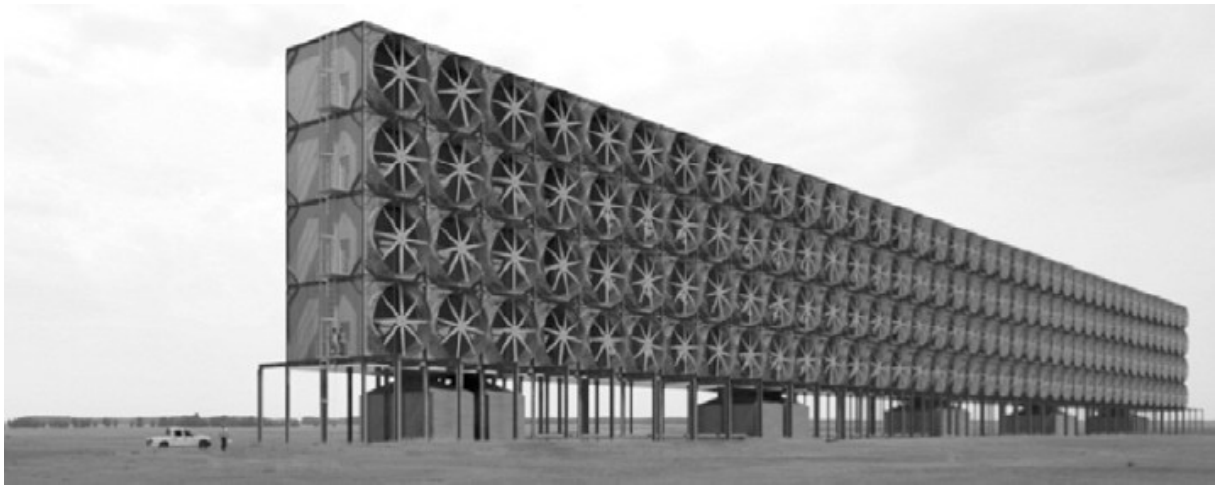

Figure 4.2 Conceptual design of the air-contactor unit, illustrating its overall geometry and modular configuration [51]

For the DAC plant considered in this study, which is designed to capture 14.2 kilotons of CO_2 per year, with an assumed design capture efficiency of 75%, the required air volumetric flow rate and corresponding inlet area were calculated to be $623\ m^3/s$ and $554\ m^2$, respectively. This results in a total of 22 sub-units, which can be arranged into a single air-contactor unit composed of two rows of 11 sub-units each, yielding overall dimensions of $10\ x\ 55\ x\ 7$ meters. Furthermore, a resulting packing volume of $2768\ m^3$ is obtained. The specific surface area available within the packing is $210\ m^2/m^3$, as adopted in the optimization model used. To accommodate the installation of fans and piping systems, the total dept of the unit is increased from the optimal packing width of 5.5 meters to 7 meters.

4.2.2. Na_2CO_3 electrolysis cell sizing

The electrochemical cell employed for the electrolysis of Na_2CO_3, which produces $NaHCO_3$, regenerates NaOH and produces H_2 and O_2 as by-products, constitutes one of the three main subsystems of the DAC process under investigation. According to *Obrist*, the operational behavior of this electrochemical cell is well understood and has been demonstrated to be scalable [10]. Nevertheless, no commercial solutions are currently available, and only limited experimental data on such electrochemical cells can be found in the literature.

For the purpose of this thesis work, the sizing of the electrochemical cell is based on experimental results reported by Liu et al., as already done to evaluate the specific energy consumption. Based on the total current calculated in Section 4.1, and assuming a current density of $120\ mA/cm^2$, at which the average experimental voltage was measured, the required active area of the electrochemical cell is estimated to be $1886\ m^2$. The total installed power, as calculated in Section 4.1, is estimated to be approximately $5953\ kW$. It is important

to note that, as previously discussed, this power requirement refers to the power required to operate the electrochemical cell, referring therefore to both DAC process and the associated hydrogen production.

The operating conditions of the electrochemical cell are assumed to be consistent with those used in the referenced experimental study. This includes the use of RuO_2/Ti as the anode material, NiMo/$NiMoO_4$ as the cathode material, and a commercial ion-exchange membrane to separate the anode and cathode compartments.

The relatively large active area required is a direct consequence of the low current density at which the electrochemical cell operates. According to a standard polarization curve, increasing the current density leads to a higher voltage requirement, which in turn increases the power consumption. However, this also reduces the necessary active surface area. Conversely, operating at a lower current density reduces both the voltage and the power requirements, but necessitates a larger active area to meet the target production rate. This relationship highlights a fundamental trade-off between power requirements and equipment size. Identifying the optimal operating point, where this trade-off is best balanced, requires detailed experimental characterization of the cell's polarization behavior. Such an investigation lies beyond the scope of this thesis, which focuses instead on a first evaluation of the overall performance of the DAC process. Therefore, the current analysis has been based on available experimental data and does not attempt to optimize the electrochemical cell's operating conditions.

Finally, it is important to note that the analysis of the Na_2CO_3 subsystem focuses exclusively on the electrochemical cell stack, while omitting the BoP components necessary for full system operation. In particular, auxiliary system required for the effective separation and handling of the gaseous by-products generated during electrolysis were not considered.

4.3. Economic analysis results

The primary objective of the economic analysis conducted for the DAC process under investigation is to estimate the CO_2 capture cost, as outlined in Section 3.4.3 (Equation 3.16). The main results, including both CAPEX and OPEX, are presented for the four subsystems into which the process has been divided: the air-contactor subsystem, the Na_2CO_3 subsystem, the NaOH concentration subsystem, and the $NaHCO_3$ thermochemical decomposition subsystem.

4.3.1. Total overnight capital

The evaluation of the TOC is based on the methodology proposed by NETL. A summary of the key parameters used in the TOC calculation is provided in Table 4.2. For conventional process components, cost estimates are obtained directly from the APEA tool. A summary of these values, referring to the conventional components in Figure 3.2, is reported in Appendix D.

Table 4.2 Methodology for the calculation of the TOC from NETL [52], [53]

Plant component	Cost (kEUR)
Component W	A
Component X	B
Component Y	C
Component Z	D
Bare Erected Cost (BEC)	A+B+C+D
Total Installation Cost (TIC)	80% BEC
Total Direct Plant Cost (TDPC)	BEC + TIC
Indirect Cost (IC)	13% TDPC
Engineering Procurement and Construction (EPC)	TDPC + IC
Contingencies & Owners' Costs (C&OC)	30% EPC
Total Overnight Capital (TOC)	EPC + C&OC

For the air-contactor and the electrochemical cell, alternative cost estimation approaches have been adopted. The component cost for the air-contactor is derived using the cost optimization model proposed by Keith et al. [44]. According to this model, the total cost of the air-contactor is divided between its two primary components: the shell and the packing. The shell cost is assumed to be proportional to the frontal area of the air-contactor unit, while the packing cost is proportional to its volume. Based on consultations with various engineering, procurement, and construction (EPC) firms, the authors report unit costs of $3700\ USD/m^2$ for the shell and $250\ USD/m^3$ for the packing. For the purposes of this analysis, these values have been adopted directly as $3700\ EUR/m^2$ and $250\ EUR/m^3$, respectively, without adjusting for currency conversion.

There is a general lack of published data regarding Na_2CO_3 electrolysis cell. As a consequence, cost data for this component is also limited. Therefore, for the purposes of this economic assessment, the cost of the electrochemical cell has been assumed to be equivalent to that of a conventional alkaline water electrolyzer, estimated at $600\ EUR/kW$ [49]. The resulting TOC for the four different subsystems is reported in Table 4.3.

Table 4.3 TOC for the four subsystems

Subsystem	TOC (kEUR)
NaOH concentration	626.4
$NaHCO_3$ decomposition	586.0
Air-contactor	7247.1
Na_2CO_3 Electrolysis	9444.4
TOTAL	17903.9

4.3.2. Operation and maintenance costs

The operation and maintenance costs are divided into fixed and variable components. Fixed costs refer to the annual expenses associated with routine maintenance of the plant, personnel wages, and insurance. For each subsystem, these costs are estimated to be 5% of TOC. Variable costs, on the other hand, represent the annual expenditures related to the consumption of utilities required for the daily operation of the plant. The utilities considered in this analysis include electricity, primarily consumed by the air-contactor and Na_2CO_3 electrolysis subsystems, thermal energy in the form of medium pressure steam, which is required by the NaOH concentration and $NaHCO_3$ thermochemical decomposition subsystems, cooling water used in the cooling units, and makeup water to compensate for process-related water losses. The cost of the solvent is not included among the utilities, as it is continuously regenerated within the process and does not require regular replenishment. Instead, its initial cost is assumed to be incorporated into the TOC of the air-contactor subsystem. Table 4.4 presents a summary of the quantities of the aforementioned utilities required to operate the overall process, reported both as normalized values per ton of CO_2 captured and on an annual basis. The annual values are those used in the evaluation of the TOC.

Table 4.4 Summary of utility consumption for the DAC process, reported per ton of CO_2 captured and on an annual basis

	Units	Value	Units	Value
Electricity	kWh_e/ton_{CO_2}	3489.5	$kWh_e/year$	49718957.3
Steam	kg_{steam}/ton_{CO_2}	2199.1	$kg_{steam}/year$	31333488.0
Cooling water	m^3/ton_{CO_2}	90.7	$m^3/year$	1291843.9
Makeup water	ton_{H_2O}/ton_{CO_2}	5.7	$ton_{H_2O}/year$	81160.8

The electricity values reported in Table 4.4 reflect the total amount required to operate the entire plant, including the full energy demand of the electrochemical cell. If only the portion of electricity strictly attributable to the DAC process were considered, excluding the share associated with hydrogen production, the electricity requirement would decrease to $970\ kWh_e/ton_{CO_2}$ or $13820576\ kWh_e/year$. However, this separation is not practically feasible, as the Na_2CO_3 electrolysis is inherently coupled with the water electrolysis reaction, and the two processes cannot be decoupled. Therefore, for the purpose of TOC evaluation, the total

electricity consumption is considered. Nonetheless, the economic analysis accounts for the potential value of the hydrogen produced as a by-product. As reported by *Obrist*, the DAC process under investigation becomes particularly attractive in scenarios with high penetration of RES, where electricity is supplied at low cost. Therefore, in this analysis, a RES electricity price of $0.01\ EUR/kWh$ is assumed [10].

The thermal energy required by the DAC process is supplied in the form of medium-pressure stream. This steam is assumed to be provided by the boiler feedwater utility of a CO_2 methanation process, modeled internally at *Shell* and based on a configuration similar to well-known Topsøe Recycle Energy-efficient Methanation Process (TREMP™). In this process, the boiler feedwater is first heated by recovering waste heat from the methanation reactors. It is then employed for process-to-process heat integration within the methanation system. Following this stage, the boiler feedwater is expanded in a turbine to generate electricity, until it reaches the desired condition of 170 ℃ and $6\ bar$, suitable for integration with the DAC process. Finally, it is proposed that this medium-pressure steam be utilized to supply the low-temperature thermal energy required by the DAC system.

According to the results of the methanation process model, the available mass flow rate of steam from a SNG plant with a production capacity of 5000 tons of CO_2 per year, when normalized per ton of CO_2 captured, corresponds to $1277.8\ kg_{steam}/ton_{CO_2}$. These results are used here to assess the potential for thermal integration with the DAC process. However, it is important to note that the detailed description of the methanation process itself falls outside the scope of this analysis and will not be discussed further. Permission has been granted to utilize the relevant outputs from this internal model for the purpose of this study.

The available steam is insufficient to fully meet the thermal energy demand of the DAC process, requiring an additional $921.3\ kg_{steam}/ton_{CO_2}$ to be supplied. For the purpose of the economic analysis, it is assumed that the fraction of steam recovered from waste heat is available at no cost, while only the additional required steam is considered a paid utility, at a cost of $0.0055\ EUR/kg_{steam}$.

Finally, utility prices of $0.1\ EUR/ton_{H_2O}$ and $0.013\ EUR/m^3$ were assumed for makeup and cooling water, respectively.

A summary of the annual variable operation and maintenance costs, based on the consumption quantities and unit prices discussed above, is presented in Table 4.5.

Table 4.5 Annual variable operational and maintenance costs based on utility consumption and unit prices

	Units	Value
Electricity	$EUR/year$	497189.6
Steam	$EUR/year$	72198.0
Cooling water	$EUR/year$	16794.0
Makeup water	$EUR/year$	8116.1

4.3.3. Capture Cost

The capture cost of the DAC process is evaluated according to the definition provided in Section 3.4.3 (Equation 3.16). For the purposes of this economic analysis, a CCF of 12.50% has been assumed. This value is consistent with the one adopted by Sabatino et al. [54] and Keith et al. [50] in the analysis of their proposed DAC process. Assuming that the plants operate for 8040 hours per year, out of a total of 8760 hours, the resulting plant availability corresponds to 92% equivalent full-load hours. However, this availability factor was already implicitly considered in the estimation of annual CO_2 capture and utility requirements, based on an operational year of 8040 hours. Consequently, for the purpose of calculating the capture cost, the parameter h_{eq} was set to 1. Based on these assumptions, a capture cost of $264.1\ EUR/ton_{CO2}$ was obtained. A breakdown of the TOC across the four main subsystems, air-contactor, Na_2CO_3 electrolysis, $NaHCO_3$ decomposition, and NaOH concentration, is presented in Table 4.6. The table also includes the levelized fixed and variable operation and maintenance costs, as well as the resulting CO_2 capture cost, all normalized per ton of CO_2 captured.

Table 4.6 Breakdown of TOC, levelized fixed and variable O&M costs, and CO_2 capture cost per subsystem

	TOC x CCF $(EUR/year)$	Levelized $C_{O\&M}^{fix}$ (EUR/ton_{CO_2})	Levelized $C_{O\&M}^{var}$ (EUR/ton_{CO_2})	Capture cost (EUR/ton_{CO_2})
Air-contactor	905886.3	25.4	3.0	92.0
Na_2CO_3 Electrolysis	1180549.8	33.1	34.9	150.9
$NaHCO_3$ decomposition	73244.3	2.1	5.5	12.7
NaOH concentration	78301.4	2.2	0.8	8.5
TOTAL	2237981.7	62.8	44.1	264.1

The capture cost presented in Table 4.6 has been evaluated by considering the total electrical energy required to actually operate the plant, which means that the full energy demand of the Na_2CO_3 electrolysis subsystem, amounting to $3489.5\ kWh_e/ton_{CO_2}$, has been used in the analysis. Regarding the thermal energy, only the portion of medium-pressure steam that must be supplied in excess of what it is assumed to be freely available from the integrated methanation process has been considered. Out of a total requirement of $2199.1\ kg_{steam}/ton_{CO_2}$, only $921.3\ kg_{steam}/ton_{CO_2}$ is therefore assumed to be externally sourced and thus results in a cost. In particular, it is assumed that the thermal energy recovered from the

methanation process is entirely allocated to meet the thermal demand of the NaOH concentration subsystem. As a result, the variable cost associated with the thermal energy for this subsystem is set to zero. The remaining portion of recovered thermal energy is directed to the $NaHCO_3$ thermochemical decomposition subsystem, and only the remaining energy to be supplied for this subsystem, which is not met by the thermal energy recovered by the integration with the methanation process is considered a paid utility and included in the cost calculation for the $NaHCO_3$ decomposition subsystem.

The capture cost associated with the air-contactor subsystem is consistent with values reported in the literature by Keith et al., which indicate a capture cost of 94 EUR per ton of CO_2 captured for the air-contactor system alone [44], which has been computed by employing the cost optimization model that they present. This same model has been employed in the present study to evaluate the capture cost of the air-contactor subsystem within the DAC process under investigation. The optimization model was originally developed for a system with a capture capacity of 1 Mt of CO_2 per year and explicitly incorporates the effects of economy of scale, which significantly reduces the overall capture cost. In contrast, to analyze the DAC process proposed in this study, a smaller capture capacity of 14.2 kilotons of CO_2 per year is assumed. Nevertheless, the same model was applied without excluding the effects associated with economies of scale. As a result, the estimated capture cost may be overly optimistic, and the actual cost at the smaller scale considered could be significantly higher.

Regarding the overall capture cost of the DAC process, it is, as expected, primarily driven by the cost associated with the Na_2CO_3 electrolysis subsystem. The high installed power and the high energy demand of the electrochemical cell operation considerably increase the total capture cost of the process. That said, when the entire process is taken into account, the production of hydrogen as a valuable by-product can help offset the associated costs, potentially making the process competitive with other DAC technologies. To try to better understand this potential, a comparison between the DAC process examined in this study and alternative DAC processes reported in the literature is presented in Section 4.4.

4.3.4. Adjusted capture cost accounting for H_2 revenue

The total electrical energy required to operate the Na_2CO_3 electrolysis subsystem has been included in the capture cost evaluation presented in Section 4.3.3. This is because it is not technically feasible to decouple the CO_2 capture process, specifically, the conversion of Na_2CO_3 to $NaHCO_3$ from the water electrolysis reaction, which simultaneously produces H_2 and O_2. Given this integration, it is reasonable to consider the potential revenue from these by-products and

assess their impact on the overall capture cost. For the purpose of this analysis, only H_2 is considered as a valuable by-product, assuming it can directly be utilized, coupled with the captured CO_2, for SNG production. However, depending on the specific application scenario, O_2 could also be valorized, and its inclusion in the economic assessment could further improve the cost-effectiveness of the process.

The amount of H_2 produced per ton of CO_2 captured is $43.6\ kg_{H_2}/ton_{CO_2}$. Assuming a hydrogen marked price of $2\ EUR/kWh$, the resulting revenue from hydrogen sales is $87.2\ EUR$ per ton of CO_2 captured. Therefore, the adjusted capture cost of the process is $176.9\ EUR$ per ton of CO_2, calculated by subtracting the hydrogen revenue from the original capture cost reported in Section 4.3.3. Although the revenue generated from hydrogen sales cannot be directly attributed to any specific subsystem, it is reasonable to associate it with the Na_2CO_3 electrolysis subsystem, as hydrogen is produced within this part of the process. As a result, the capture cost attributed to the Na_2CO_3 electrolysis subsystem decreases to $63.7\ EUR/ton_{CO_2}$, as shown in Table 4.7. As can be seen in the table, when compared with Table 4.6, the only differences are the reduced capture cost of the Na_2CO_3 electrolysis subsystem and the resulting adjusted capture cost, while all other values remain unchanged.

Table 4.7 Breakdown of TOC, levelized fixed and variable O&M costs, and CO_2 capture cost per subsystem, including revenues from H_2 selling

	TOC x CCF $(EUR/year)$	Levelized $C_{O\&M}^{fix}$ (EUR/ton_{CO_2})	Levelized $C_{O\&M}^{var}$ (EUR/ton_{CO_2})	Adjusted Capture cost (EUR/ton_{CO_2})
Air-contactor	905886.3	25.4	3.0	92.0
Na_2CO_3 Electrolysis	1180549.8	33.1	34.9	63.7
$NaHCO_3$ decomposition	73244.3	2.1	5.5	12.7
NaOH concentration	78301.4	2.2	0.8	8.5
TOTAL	2237981.7	62.8	44.1	176.9

4.3.5. Impact of parameters variation on capture cost

The estimation of the overall capture cost and the adjusted capture cost was carried out by considering the TOC as well as the fixed and variable O&M costs of the system. The TOC was evaluated following the methodology proposed by the NETL. This evaluation began with the bare equipment costs, which were obtained using the APEA tool for conventional components, the already largely discussed optimization model for the air-contactor subsystem, and literature data on the capital cost of state-of-the-art alkaline water electrolysis stacks for the Na_2CO_3 electrolysis subsystem, due to the lack of specific cost data for Na_2CO_3 electrolysis cell. Fixed O&M costs were estimated as a percentage of the TOC, while variable O&M costs were obtained from information present in the literature. However, several of the parameters used in this analysis

are subject to inherent uncertainty. Assumptions such as the cost of electricity or the installation cost of the electrochemical cell can significantly influence the final capture cost. Therefore, to assess the sensitivity of the capture cost to variation in these parameters, a sensitivity analysis has been conducted as the concluding step of this preliminary economic assessment of the DAC process under study.

The parameters selected for the sensitivity analysis are: electricity price, installation cost of the electrochemical cell, CCF, and the market price of hydrogen. To estimate the capture cost, the electricity price was assumed to be equal to $0.01\ EUR/kWh$. However, this value remains challenging to achieve under current market conditions and is typically attainable only in specific countries and with favorable financial frameworks. Consequently, it is important to understand how variations in electricity price influence the overall capture cost.

The installation cost of the electrochemical cell was assumed to be equivalent to that of state-of-the-art alkaline water electrolyzer. This assumption intrinsically introduces uncertainty, thereby justifying the inclusion of this parameter in the sensitivity analysis. Moreover, the cost data available in the literature for alkaline water electrolyzers is significantly influenced by the scale of installation, due to economies of scale that reduce costs at larger capacities. Given the relatively small capacity of the electrochemical cell considered in this study, higher installation costs may be expected. This further supports the need for sensitivity analysis on this parameter.

Regarding the CCF, the value was directly adopted from literature sources that analyze other DAC processes [50], [54]. However, the CCF is a complex parameter to estimate, which includes several assumptions and financial considerations related to the economic scheme of the plant. Therefore, it is important to evaluate how variations in the CCF could affect the capture cost.

For the hydrogen market price, a reference value of $2\ EUR/kg_{H_2}$ was assumed to estimate the potential revenue from hydrogen sale or, alternatively, the cost saving from internal hydrogen use, if, for instance, the DAC process is intended to be coupled with a CO_2 methanation process. Although the hydrogen produced in this process can be classified as renewable, obtained from water electrolyzer powered by RES, the assumed price is comparable to that of gray hydrogen produced via steam methane reforming [55]. However, given that the cost of renewable hydrogen is expected to decrease in the near future [56], it is important to understand how such a decrease could impact the capture cost and, consequently, the economic viability of the DAC process under investigation.

Electricity cost, installation cost of the electrochemical cell, and the CCF all have a direct correlation with the capture cost, i.e., an increase in any of these parameters leads to a higher capture cost. Conversely, a decrease in the hydrogen market price leads to an increase in the capture cost, by reducing potential revenue or cost savings. Due to the optimistic nature of the values assumed for these parameters, for the evaluation of the capture cost presented in Sections 4.3.3 and 4.3.4, which define the base case scenario, a unidirectional sensitivity analysis was conducted, focusing on the impact of increasing electricity price, electrochemical cell installation cost, and CCF, as well as the effect of decreasing hydrogen market price.

Other parameters, such as the cost of medium-pressure steam utilized to supply the thermal energy, or the cost of makeup and cooling water, are not expected to undergo significant fluctuations. As such they were not included in this sensitivity analysis.

Figure 4.3 presents the results of the sensitivity analysis. As previously discussed, increases in the Na_2CO_3 electrolysis installation cost, electricity price and CCF, represented on the primary horizontal axis, lead to a corresponding increase in the adjusted capture cost. Similarly, a decrease in the H_2 market price, shown on the secondary horizontal axis, also results in a higher adjusted capture cost. A key aspect of this analysis is the comparison of the slopes of the curves, which provides an understanding of how variations in each parameter influence the adjusted capture cost. A steeper slope indicates a greater sensitivity, while a gentler slope indicates a lesser impact. Among the parameter analyzed, the CCF exhibits the steepest slope, resulting in 44% increase in the adjusted capture cost for a 50% increase in CCF, indicating that it has the most significant influence. This is expected, as the CCF directly multiplies the TOC, thereby amplifying its effect on the final capture cost. Therefore, obtaining an accurate estimate of CCF is of primary importance to avoid unforeseen increases in capture costs. Despite the high electricity demand of the process, variations in electricity price have the least impact on the adjusted capture cost among the parameters considered, with a 11% increase in capture cost observed for a 50% rise in electricity price. Changes in the Na_2CO_3 electrolysis installation cost and the hydrogen market price have a greater effect than electricity price fluctuations, but less than that of the CCF. The installation cost of Na_2CO_3 electrolysis system has a more pronounced impact than a reduction in the hydrogen market price.

Conversely, an increase in the hydrogen market price leads to a corresponding decrease in the adjusted capture cost. For instance, assuming a hydrogen market price of $5\ EUR/kg_{H_2}$, the adjusted capture cost decreases to $45.9\ EUR/ton_{CO_2}$. Notably, a hydrogen market price of $6.05\ EUR/kg_{H_2}$ would reduce the adjusted capture cost to zero. In contrast, if the hydrogen

market price drops to zero, meaning no revenue is generated from hydrogen sales, the adjusted capture cost remains equal to the original capture cost, as no offsetting benefit is realized.

Considering a more realistic scenario, where the electricity price is set to $0.06\ EUR/kWh$, consistent with values adopted in the analysis of other DAC processes [50], [54], and the CCF and hydrogen market price are maintained as defined in Sections 4.3.3 and 4.3.4, a capture cost and adjusted capture cost of $450.4\ EUR/ton_{CO_2}$ and $363.2\ EUR/ton_{CO_2}$, respectively, are achieved. This scenario can be considered more representative of current conditions, due to the adoption of more realistic electricity price.

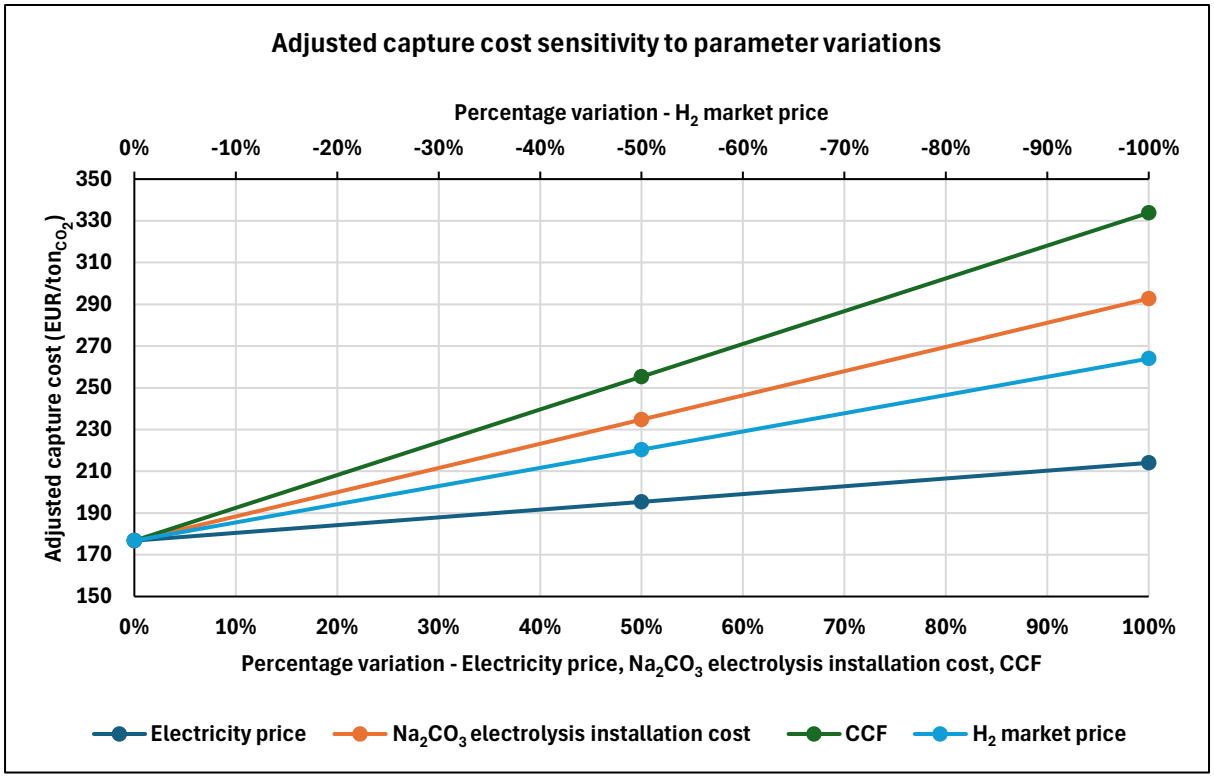

Figure 4.3 Adjusted capture cost response to changes in electricity price, Na_2CO_3 electrolysis installation cost, CCF and H_2 market price

4.4. Comparison with other DAC processes

A specific energy consumption of approximately $1200\ kWh_e/ton_{CO_2}$ and $1400\ kWh_t/ton_{CO_2}$ was obtained when considering the DAC process alone. However, when accounting for the total energy demand required to operate the Na_2CO_3 electrolysis subsystem, the actual electrical energy consumption increases significantly to $3489.5\ kWh_e/ton_{CO_2}$. Despite this, the calculated CO_2 capture cost remains promising, amounting to $264.1\ EUR/ton_{CO2}$ in the base case scenario. This cost further decreases to $176.9\ EUR/ton_{CO_2}$, when revenue from hydrogen

sales is included. In a scenario where the electricity price is assumed to be $0.06\ EUR/kWh$, the capture cost and the adjusted capture cost are estimated at $450.4\ EUR/ton_{CO_2}$ and $363.2\ EUR/ton_{CO_2}$, respectively.

To assess the competitiveness of these results, a comparative analysis with other DAC technologies is proposed. Specifically, two alternative DAC processes are considered: the system developed by *CE* [50], and the electrochemical DAC process investigated by Sabatino et al. [54]. The *CE* process is based on the approach described in Section 2.1.1 (Reactions 2.4–2.7), wherein NaOH is replaced by potassium hydroxide (KOH), and relies entirely on thermal regeneration, requiring high-temperature heat. In contrast, the process proposed by Sabatino et al. employs the same 'loading' phase, using an aqueous KOH solution, but features a fully electrochemical 'unloading' phase. This phases utilizes a two-compartment BPMED cell for the simultaneous regeneration of the solvent and CO_2 release.

The process analyzed in this thesis, represents a hybrid approach that combines electrochemical and thermal steps, requiring only low-temperature thermal energy. This configuration may offer a favorable compromise, leveraging relatively mature and scalable technologies. One of the key advantage of the *Obrist* process over the *CE* system is its independence from high-temperature heat, enabling operation using electricity from RES alone. This aligns well with ongoing efforts to phase out fossil fuels and electrification trend. Although the process proposed by Sabatino et al. also relies solely on electricity, its current low technology readiness level and the high cost of BPMED membranes, as noted by the authors, may hinder its scalability and commercial viability in the near term. Furthermore, the added advantage of the production of H_2 as useful by-product in the *Obrist* process may make this approach more attractive for implementation, particularly in scenarios where the DAC system is directly integrated with processes that require both CO_2 and H_2 as feedstock molecules, such as CO_2 methanation.

The overall process proposed by *CE* requires a total energy input of $8.81\ GJ$ of natural gas per ton of CO_2 captured, or $5.25\ GJ$ of natural gas and $366\ kWh$ of electricity, per ton of CO_2 captured, including compression of the captured CO_2 to $15\ MPa$. In contrast, the analysis conducted by Sabatino et al., focuses primarily on assessing the possible advantage of the electrochemical 'unloading' phase using BPMED, assuming the same air-contactor design as CE. Under the optimal conditions defined by a trade-off between current density, current efficiency, solution composition and operating pressure, the lowest energy requirement for regeneration alone reported is $236\ kJ/mol_{CO_2}$ or $1489\ kWh/ton_{CO_2}$. However, this values correspond to low current densities. To minimize capture cost, aiming at the optimal trade-off between capital

expenditure and operational expenditure, a higher energy demand of $957\ kJ/mol_{CO_2}$ or $6038\ kWh/ton_{CO_2}$ is used, which reflects a more realistic operating point. This value accounts for the BPMED cell operation, excluding the air-contactor, which is assumed to be the same as in the *CE* process, consistent also with the approach adopted in this thesis.

Due to differences in energy sources and the inclusion of CO_2 compression to $15\ MPa$ in the *CE* and Sabatino et al. processes, an aspect not considered in this thesis, as CO_2 pre-treatment is assumed to be part of the methanation process, a direct comparison of specific energy requirements is not straightforward. Nevertheless, a summary of the specific energy demand for the three processes under comparison is presented in Table 4.8. The values reported for the *CE* and Sabatino et al. processes include the energy required for the entire CO_2 capture process, including compression to $15\ MPa$. In contrast, the value indicated for the process analyzed in this thesis reflects only the energy demand of the capture process itself, excluding CO_2 compression.

Table 4.8 Specific energy demand for the three processes under comparison

		CE	**This work**	**Sabatino et al.**
Electrical energy	kWh_e/ton_{CO_2}	366	3728	6254,3
Low temperature thermal energy, up to 140 °C	kWh_t/ton_{CO_2}	0	1392,1	0
Natural Gas	GJ/ton_{CO_2}	5,25	0	0

Therefore, a more meaningful basis for comparison is the capture cost. The capture cost for the *CE* process, evaluated with the same methodology followed for this thesis work, ranges from 94 to $232\ EUR/ton_{CO_2}$, depending on operating conditions and assumptions. In one of the representative scenarios assumed by the authors, which considers an energy demand of $5.25\ GJ$ of natural gas and $366\ kWh$ of electricity per ton of CO_2, a CCF of 12.50%, an electricity price of $0.06\ EUR/kWh$, and CO_2 delivery at $15\ MPa$, the capture cost is estimated at $163\ EUR/ton_{CO_2}$.

For the Sabatino et al. process, under the same assumptions (CCF of 12.50%, electricity price of $0.06\ EUR/kWh$, CO_2 compression to $15\ MPa$), and considering specific energy consumption for the BPMED cell of $263\ kJ/ton_{CO_2}$, the total capture cost is estimated at $773\ EUR/ton_{CO_2}$. This high cost is primarily driven by the substantial electricity demand and membrane replacement costs, which significantly impact fixed operation and maintenance expenses.

Under equivalent conditions (CCF of 12.50%, electricity price of $0.06\ EUR/kWh$), the adjusted capture cost for the process analyzed with this thesis work, not including the CO_2 compression, is $363.2\ EUR/ton_{CO_2}$. The adjusted cost, including the revenue from hydrogen selling, has been

considered, instead of the normal capture cost, due to the inclusion of the actual energy required to operate the Na_2CO_3 electrolysis cell in the cost calculation. If the electricity price is reduced to $0.01\ EUR/kWh$, the adjusted capture cost drops to $176.9\ EUR/ton_{CO_2}$.

As previously discussed, CO_2 compression to $15\ MPa$ is not included in the process evaluated in this thesis. However, to enable a more uniform comparison with the *CE* and Sabatino et al. processes, ad additional cost of $22.2\ EUR/ton_{CO_2}$, derived from the results reported by Sabatino et al., can be added to account for CO_2 compression. This adjustment results in a total capture cost of $385.4\ EUR/ton_{CO_2}$ under the same conditions used for the other two processes (i.e., CCF of 12.50%, electricity price of $0.06\ EUR/kWh$, and CO_2 compression to $15\ MPa$). The capture costs of the three processes under these harmonized conditions are summarized in Figure 4.4, which provides a visual comparison to complement the numerical data.

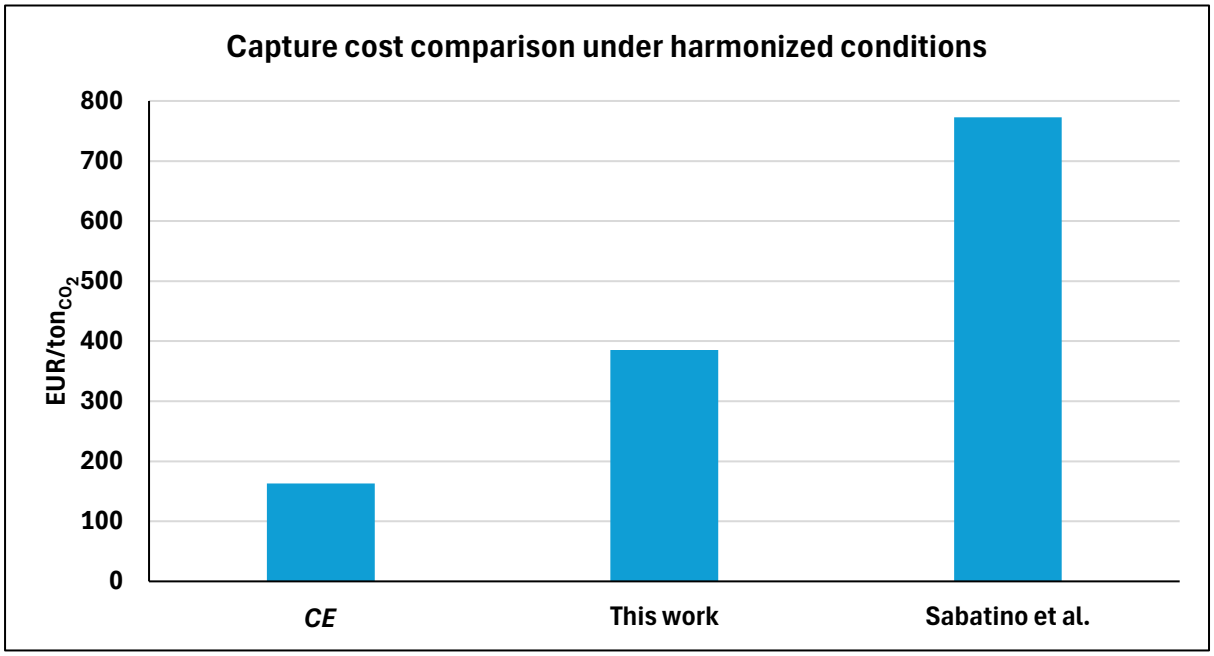

Figure 4.4 Capture cost of the three processes compared under harmonized conditions

As shown, the capture cost of the process investigated in this thesis lies between that of the *CE* and Sabatino et al. processes, suggesting that it offers balanced compromise not only in terms of technological maturity and energy input sources, but also in terms of economic feasibility. This hybrid approach may support the accelerated development and commercialization of DAC technologies, particularly in scenarios where reliance on fossil fuels is to be eliminated.

5.Conclusions

This thesis presented a simulation-based evaluation of a novel DAC system that integrates electrochemical and thermochemical processes, as proposed by *Obrist*. The system offers several key advantages, including the production of valuable by-products such as H_2 and O_2, a primary reliance on electricity, facilitating integration with RES, and low-temperature thermal energy requirement, which enables coupling with waste heat recovery solutions. The primary objective of this work was to assess the energy requirements and economic feasibility of the proposed process.

The system was modeled using *Aspen Plus* and designed to support a CO_2 methanation process with an annual SNG production of $5000\ tons$. This corresponds to a CO_2 capture rate of 14.2 kilotons per year and a simultaneous hydrogen production of 621 tons per year. The simulation results indicated that the DAC process alone requires approximately $1200\ kWh_e/ton_{CO_2}$ of electrical energy and $1400\ kWh_t/ton_{CO_2}$ of low-temperature thermal energy. When the full energy demand of the electrochemical cell, including hydrogen production, is considered, the total electrical energy required increases to $3489.5\ kWh_e/ton_{CO_2}$.

The economic analysis estimated a capture cost of $264.1\ EUR/ton_{CO_2}$. When accounting for revenue from hydrogen by-product sales, the adjusted capture cost decreases to $176.9\ EUR/ton_{CO_2}$. A sensitivity analysis revealed that the CCF has the most significant impact on capture cost, followed by the installation cost of the electrochemical cell and the market price of hydrogen.

Compared to other DAC processes, the *Obrist* system offers a promising balance between energy efficiency, scalability, and economic viability. It supports the accelerated development and deployment of DAC technologies, particularly in applications where both CO_2 and H_2 are required.

Several opportunities exist to extend and refine the work presented in this thesis. First, the boundaries of the analysis could be expanded to include electricity production, hydrogen production, and the methanation process, enabling a more comprehensive assessment of the overall SNG production route. Further research should also focus on improving the understanding of the electrochemical cell's behavior and identifying optimal operating conditions, particularly in terms of current density, which affects both energy consumption and the required active surface area, thereby influencing the trade-off between operational and

capital expenditures. The NaOH/Na_2CO_3 separation subsystem, which was excluded due to modeling limitations and lack of established methods, should be further investigated to quantify its energy and cost implications. Additionally, the current heat integration strategy, based on trial-and-error approach, could be enhanced through the application of a systematic pinch analysis to optimize thermal energy recovery and minimize external heat demand.

The process analyzed in this thesis represents a technically and economically viable approach for atmospheric CO_2 removal, particularly in scenarios were reducing dependence on fossil fuels and increasing reliance of electricity from RES as the primary energy input is essential. With further development and optimization, it could play a significant role in achieving climate targets and advancing the transition to a low-carbon economy. Importantly, the process has the potential to accelerate the development and commercialization of DAC technologies. This is largely due to its reliance on well-established electrochemical and thermochemical processes, which are already mature and scalable. By building on these proven technologies, the *Obrist* approach offers a practical and realist pathway toward large-scale deployment of DAC systems, provided that the remaining technical challenges are addressed through continued research and pilot-scale validation.

Appendix A – PFD of the process with the subsystems highlighted

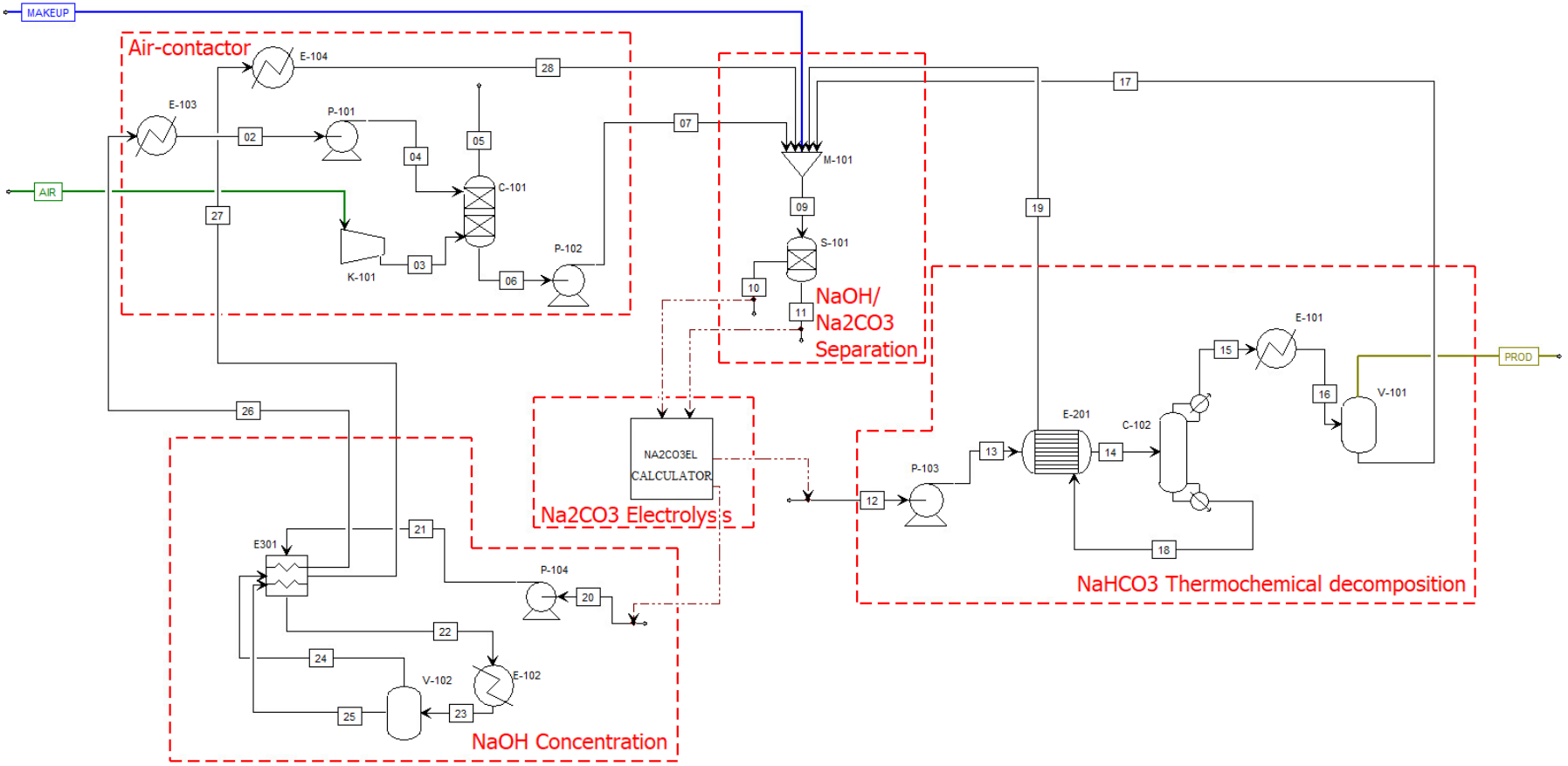

Appendix B – Streams table

	AIR	2	3	4	5	6	7	MAKEUP
Temperature, °C	25,0	40,0	25,4	40,0	20,7	20,5	20,5	25,0
Pressure, bar	1,01	1,01	1,01	1,02	1,01	1,01	1,11	1,11
Mole Flows, kmol/h	132030,0	1680,0	132030,0	1680,0	132555,0	1113,3	1113,3	685,0
Mole Fractions								
N_2	0,77528	0	0,77528	0	0,77221	0,00000	0,00000	0
O_2	0,20547	0	0,20547	0	0,20465	0,00000	0,00000	0
CO_2	0,00042	0	0,00042	0	0,00010	0,00000	0,00000	0
H_2O	0,01884	0,90476	0,01884	0,90476	0,02304	0,89064	0,89064	1,00000
NaOH	0	0	0	0	0	0	0	0
Na_2CO_3	0	0	0	0	0	0	0	0
$NaHCO_3$	0	0	0	0	0	0	0	0
H_2	0	0	0	0	0	0	0	0
H^+	0	0,00000	0	0,00000	0	0,00000	0,00000	0,00000
NA^+	0	0,04762	0	0,04762	0	0,07186	0,07186	0
HCO_3^-	0	0	0	0	0	0,00311	0,00311	0
OH^-	0	0,04762	0	0,04762	0	0,00001	0,00001	0,00000
CO_3^{2-}	0	0	0	0	0	0,03437	0,03437	0

	9	10	11	12	13	14	15	16
Temperature, °C	33,5	33,5	33,5	46,0		109,0	95,0	40,0
Pressure, bar	1,11	1,11	1,11	1,11	3,50	3,00	1,51	1,11
Mole Flows, kmol/h	2983,3	363,9	2619,3	796,8	796,8	818,3	92,3	92,3
Mole Fractions								
N_2	0,00000	0,00001	0	0	0	0	0	0
O_2	0,00000	0,00001	0	0	0	0	0	0
CO_2	0,00000	0,00000	0	0,00234	0,00234	0,02856	0,43662	0,43662
H_2O	0,91690	0,31890	1,00000	0,79115	0,79116	0,79664	0,56338	0,56338
NaOH	0	0	0	0	0	0	0	0
Na_2CO_3	0	0	0	0	0	0	0	0
$NaHCO_3$	0	0	0	0	0	0	0	0
H_2	0	0	0	0	0	0	0	0
H^+	0,00000	0,00000	0,00000	0,00000	0,00000	0,00000	0	0,00000
NA^+	0,05471	0,44845	0	0,10442	0,10442	0,10168	0	0
HCO_3^-	0,00207	0,01681	0	0,09975	0,09974	0,04456	0	0,00000
OH^-	0,00002	0,00000	0,00000	0,00000	0,00000	0,00001	0	0,00000
CO_3^{2-}	0,02631	0,21582	0	0,00234	0,00234	0,02855	0	0,00000

	17	18	19	20	21	22	23	24
Temperature, °C	40,0	139,0	54,6	46,0	46,0	131,5	131,7	131,7
Pressure, bar	1,11	3,00	2,50	1,11	3,11	2,61	2,61	2,61
Mole Flows, kmol/h	49,1	742,9	742,9	2073,0	2073,0	2073,0	2073,0	393,0
Mole Fractions								
N_2	0	0	0	0	0	0	0	0
O_2	0	0	0	0	0	0	0	0
CO_2	0,00044	0,00001	0,00000	0	0	0	0	0
H_2O	0,99955	0,82987	0,83023	0,92282	0,92282	0,92282	0,92282	1,00000
NaOH	0	0	0	0	0	0	0	0
Na_2CO_3	0	0	0	0	0	0	0	0
$NaHCO_3$	0	0	0	0	0	0	0	0
H_2	0	0	0	0	0	0	0	0
H^+	0,00000	0,00000	0,00000	0,00000	0,00000	0,00000	0,00000	0
NA^+	0	0,11199	0,11199	0,03859	0,03859	0,03859	0,03859	0
HCO_3^-	0,00000	0,00391	0,00355	0	0	0	0	0
OH^-	0,00000	0,00039	0,00003	0,03859	0,03859	0,03859	0,03859	0
CO_3^{2-}	0,00000	0,05385	0,05420	0	0	0	0	0

	25	26	27	28	PROD
Temperature, °C	131,7	70,0	70,0	40,0	40,0
Pressure, bar	2,61	2,11	2,11	1,11	1,11
Mole Flows, kmol/h	1680,0	1680,0	393,0	393,0	43,2
Mole Fractions					
N_2	0	0	0	0	0
O_2	0	0	0	0	0
CO_2	0	0	0	0	0,93254
H_2O	0,90476	0,90476	1,00000	1,00000	0,06746
NaOH	0	0	0	0	0
Na_2CO_3	0	0	0	0	0
$NaHCO_3$	0	0	0	0	0
H_2	0	0	0	0	0
H^+	0,00000	0,00000	0,00000	0,00000	0
NA^+	0,04762	0,04762	0	0	0
HCO_3^-	0	0	0	0	0
OH^-	0,04762	0,04762	0,00000	0,00000	0
CO_3^{2-}	0	0	0	0	0

Appendix C – Design specifications of conventional equipment

No. Pump	Service	Capacity		Pressure discharge (bar)	Head developed (m liquid)	Pumping temp. (°C)	Density at pumping temp. (kg/m³)	Estimated required power (W)	Installed power (W)
		Normal flow (m³/h)	Maximum flow (m³/h)						
P-102	C-101 outlet NaOH pump	3,46	3,81	1,11	0,53	16	1935,0	11,3	12,4
P-103	C-102 inlet NaHCO3 pump	14,20	15,62	3,5	18,90	46	1289,4	1109,3	1220,2
P-104	V-102 inlet NaOH pump	34,69	38,15	3,11	18,78	46	1085,8	2267,0	2493,7

No. Column	Service	Design temp. (°C)	Design pressure (bar)	Size dia. x length (mm)	Feed gas flow (Nm³/h)
C-102	NaHCO3 decomp.	140	3	600x4900	406,74

No. Heat exchanger	Service	Duty (kW)	Total (bare) outside surface (m²)	Design conditions			
				Hot side		Cold side	
				Temp (°C)	Pressure (bar)	Temp (°C)	Pressure (bar)
E-101	CO2 product utility water	-641,3	17,6	122,8	1,51	35	1,0
E-102	NaOH solution lean utility steam	1070,4	35,1	187,8	2,61	159,5	6,0
E-103	NaOH solution conc. utility water	-976,4	42,8	121,1	2,11	35	1,0
E-104	recovery water utility water	-246,9	10,8	121,1	2,11	35	1,0
E-201	C-102 inlet C-102 outlet	1328,3	82,8	166,8	3,0	109	3,5
E-301	NaOH solution lean NaOH solution conc. recovery water	6830,8	523,2	1) 131,7 2) 131,7	2,61 2,61	46	3,11
E-reb	C-102 outlet utility steam	1395,5	60,2	166,8	6,0	139	3,0

No. Vessel	Service	Design temp. (°C)	Design pressure (bar)	Size dia. x length (mm)	Remarks
V-101	CO2/water separation	40	1,11	800x2300	Vertical GL separator
V-102	NaOH concentration	130	2,61	1800x5000	Vertical GL separator

Appendix D – Convetional process equipment cost

Equipment	Cost (EUR)
P-104	7600
E-102	21100
E-103	23300
E-104	14700
E-301	137400
V-102	32800
P-103	6400
E-201	35600
C-102	140100
E-101	17400
V-101	22100

Annex I – Sustainability report

In the following paragraphs, a brief discussion concerning the sustainability of the developed thesis work is presented. In particular, the focus of the analysis will be on discussing the environmental and economic sustainability of the work, along with brief overview of the ethical implications and relationship of it with the Sustainable Development Goals (SDGs).

I.I Environmental sustainability

A first estimation of the environmental impact of this thesis work can be assessed by considering and quantifying the energy consumed during the research activities, together with the associated emissions. The thesis project was developed over a period of 18 weeks, working full-time from 8 a.m. to 6 p.m., with a total of 1.5-hour breaks, at the Energy Transition Campus Amsterdam (ETCA), in the Netherlands. Most of the work was conducted using a laptop, two external monitors, and a remote desktop located at the Politecnico di Torino in Italy. The laptop was primarily used to operate *Shell*'s internal software and to perform common office productivity tasks such as browsing the web, using word processors, and checking emails. The remote desktop was used to operate with the *Aspen Plus* software. To quantify the consumed energy and the associated emissions, the following assumptions were made:

- The average power consumption is 65 W for the laptop [57], 48 W for each external monitor [58], and 120 W for the remote desktop operated through a virtual machine [59].
- The laptop and the two external monitors were used for 90% of the total working hours.
- The remote desktop was used for 30% of the total working hours.
- The estimated number of browser queries is 50 per hour, each with a carbon intensity of 0.2 g CO_2-equivalent per query [60].
- The estimated number of Copilot queries is 1 per hour, each with a carbon intensity of 4.32 g CO_2-equivalent per query [60].
- The carbon intensity of electricity generation is assumed to be 268 g CO_2-equivalent/kWh in the Netherlands and 331 g CO_2-equivalent/kWh in Italy [61].

Based on these assumptions, the total energy consumption is estimated to be 111 kWh in the Netherlands and 28 kWh in Italy, resulting in a total CO_2-equivalent emission of approximately 50 kg.

In addition to the emissions from energy consumption during research activities, it is important to account for emissions related to travel and commuting. For travel, this includes the initial flight

from Barcelona (BCN) to Amsterdam (AMS) at the beginning of the internship, as well as a round-trip flight from AMS to BCN. The latter was necessary to return for the thesis defense and then come back to AMS, as the internship had not yet concluded. The distance between Barcelona and Amsterdam is approximately 1,240 km one way, totaling 3,720 km for all flights. Using an emission factor of 0.151 kg CO_2-equivalent per passenger-kilometer [62], the total emissions from air travel amount to approximately 561 kg CO_2-equivalent.

Commuting emissions were minimal, as the daily route was made by bicycle. However, an important part of the commute involved taking the ferry connecting Amsterdam Central Station with Amsterdam North (Buiksloterweg), part of the GVB ferry network. These electric ferries produce zero direct CO_2 emissions but consume electricity from the grid. Assuming an energy consumption of 0.2 kWh per passenger per trip and the Dutch grid emission factor reported before, the estimated indirect emissions are 0.0536 kg CO_2 per trip. Given that the ferry was taken twice per day over 5 workdays per week for 18 weeks (180 total trips), this results in approximately 10 kg CO_2-equivalent for commuting by ferry.

Considering energy consumption (50 kg), air travel (561 kg), and commuting by ferry (10 kg), the total estimated CO_2-equivalent emissions associated with this thesis work amount to approximately 621 kg.

I.II Economic sustainability

The economic sustainability of the thesis work can be evaluated by considering material and human resources. Among the material resources, software-related costs were limited. The only software requiring a license was *Aspen Plus*, which was accessed through a virtual machine shared with other students. This shared usage significantly reduces the economic impact. All other software tools employed during the project were internally developed by *Shell*, further minimizing software-related expenses.

Regarding hardware, the project was conducted using a company-provided laptop, which was a refurbished second-hand device. This choice helped lower both the environmental footprint and financial cost associated with hardware.

The human resources involved in this project include my own time spent working on the thesis, as well as the time of my supervisors who provided guidance and feedback throughout the process. While my time investment is an important cost to consider, it is crucial to note that the project contributes to my academic and professional development, which in turn may lead to significant future benefits both economically and socially.

These considerations, while relevant, are just a few examples of the many factors that would be part of a comprehensive economic sustainability analysis. However, a detailed breakdown is beyond the scope of this brief overview of the project's sustainability.

I.III Ethical implications

The thesis contributes to the development of DAC technology, which aims to reduce the concentration of CO_2 in the atmosphere. This aligns with the ethical imperative to mitigate climate change by developing technologies that support environmental sustainability. The research adheres to the ethical codes of conduct for engineering and scientific research, which emphasize the importance of accuracy, objectivity, and responsibility. The work was conducted with the goal of advancing knowledge in the field of sustainable energy and contributing to the global efforts to combat climate change.

I.IV Relationship with the SDGs

This thesis supports several United Nations SDGs, adopted in 2015 to address global challenges [63]. It contributes to SDG 7 (Affordable and Clean Energy) by promoting the integration of DAC with green hydrogen production, offering cleaner energy solutions for power and transportation. In line with SDG 9 (Industry, Innovation, and Infrastructure), the research advances innovative technologies for large-scale CO_2 capture and green hydrogen generation, supporting the development of sustainable energy infrastructure. It also aligns with SDG 12 (Responsible Consumption and Production) by fostering a circular economy approach, capturing CO_2 and potentially converting it into valuable products, thereby improving resource efficiency. Finally, the core objective of reducing atmospheric CO_2 directly supports SDG 13 (Climate Action), contributing to global efforts to combat climate change. Overall, the work undertaken in this thesis addresses critical sustainability challenges through technological innovation and environmental responsibility.

References

[1] M. McNutt, “Climate change impacts,” *Science (1979)*, vol. 341, no. 6145, p. 435, Aug. 2013, doi: 10.1126/SCIENCE.1243256/ASSET/293A1C33-F006-4627-AF78-F13A2A65236E/ASSETS/GRAPHIC/341_435_F2.JPEG.

[2] J. Hansen, M. Sato, R. Ruedy, K. Lo, D. W. Lea, and M. Medina-Elizade, “Global temperature change,” *Proc Natl Acad Sci U S A*, vol. 103, no. 39, pp. 14288–14293, Sep. 2006, doi: 10.1073/PNAS.0606291103/SUPPL_FILE/06291FIG9.PDF.

[3] “THE PARIS AGREEMENT,” 2016, Accessed: Feb. 18, 2025. [Online]. Available: https://treaties.un.org/Pages/ViewDetails.aspx?src=TREATY&mtdsg_no=XXVII-7-

[4] “The Paris Agreement | UNFCCC.” Accessed: Feb. 18, 2025. [Online]. Available: https://unfccc.int/process-and-meetings/the-paris-agreement

[5] K. O. Yoro and M. O. Daramola, “CO2 emission sources, greenhouse gases, and the global warming effect,” *Advances in Carbon Capture: Methods, Technologies and Applications*, pp. 3–28, Jan. 2020, doi: 10.1016/B978-0-12-819657-1.00001-3.

[6] M. M. Miralles-Quirós and J. L. Miralles-Quirós, “Decarbonization and the Benefits of Tackling Climate Change,” *International Journal of Environmental Research and Public Health 2022, Vol. 19, Page 7776*, vol. 19, no. 13, p. 7776, Jun. 2022, doi: 10.3390/IJERPH19137776.

[7] E. S. Sanz-Pérez, C. R. Murdock, S. A. Didas, and C. W. Jones, “Direct Capture of CO2 from Ambient Air,” *Chem Rev*, vol. 116, no. 19, pp. 11840–11876, Oct. 2016, doi: 10.1021/ACS.CHEMREV.6B00173/ASSET/IMAGES/LARGE/CR-2016-00173P_0028.JPEG.

[8] K. Lackner, “Carbon Dioxide Extraction from Air: Is It An Option?,” Jan. 01, 1999. Accessed: Feb. 18, 2025. [Online]. Available: https://www.academia.edu/120690670/Carbon_Dioxide_Extraction_from_Air_Is_It_An_Option

[9] “OBRIST Group - Sustainable, emission reducing innovations.” Accessed: Feb. 18, 2025. [Online]. Available: https://www.obrist.at/

[10] "Cutting-Edge CO2 Reduction: Exploring Direct Air Capture Technology | Obrist Webinar - YouTube." Accessed: Feb. 18, 2025. [Online]. Available: https://www.youtube.com/watch?v=pbB7YddjHJs

[11] M. Wang, A. Lawal, P. Stephenson, J. Sidders, and C. Ramshaw, "Post-combustion CO2 capture with chemical absorption: A state-of-the-art review," *Chemical Engineering Research and Design*, vol. 89, no. 9, pp. 1609–1624, Sep. 2011, doi: 10.1016/J.CHERD.2010.11.005.

[12] R. S. Haszeldine, S. Flude, G. Johnson, and V. Scott, "Negative emissions technologies and carbon capture and storage to achieve the Paris Agreement commitments," *Philosophical Transactions of the Royal Society A: Mathematical, Physical and Engineering Sciences*, vol. 376, no. 2119, May 2018, doi: 10.1098/RSTA.2016.0447.

[13] Z. Zolfaghari, A. Aslani, A. Moshari, and M. Malekli, "Direct air capture from demonstration to commercialization stage: A bibliometric analysis," *Int J Energy Res*, vol. 46, no. 1, pp. 383–396, Jan. 2022, doi: 10.1002/ER.7203.

[14] A. Sanna, M. Uibu, G. Caramanna, R. Kuusik, and M. M. Maroto-Valer, "A review of mineral carbonation technologies to sequester CO 2," *Chem Soc Rev*, vol. 43, no. 23, pp. 8049–8080, Nov. 2014, doi: 10.1039/C4CS00035H.

[15] E. S. Sanz-Pérez, C. R. Murdock, S. A. Didas, and C. W. Jones, "Direct Capture of CO2 from Ambient Air," *Chem Rev*, vol. 116, no. 19, pp. 11840–11876, Oct. 2016, doi: 10.1021/ACS.CHEMREV.6B00173/ASSET/IMAGES/LARGE/CR-2016-00173P_0028.JPEG.

[16] S. A. Didas, S. Choi, W. Chaikittisilp, and C. W. Jones, "Amine-Oxide Hybrid Materials for CO2 Capture from Ambient Air," *Acc Chem Res*, vol. 48, no. 10, pp. 2680–2687, Oct. 2015, doi: 10.1021/ACS.ACCOUNTS.5B00284/SUPPL_FILE/AR5B00284_SI_001.PDF.

[17] K. Lackner, H.-J. Ziock, and P. Grimes, "Carbon Dioxide Extraction from Air: Is It An Option?," Feb. 01, 1999.

[18] M. Ragnar, G. Henriksson, M. E. Lindström, M. Wimby, J. Blechschmidt, and S. Heinemann, "Pulp," *Ullmann's Encyclopedia of Industrial Chemistry*, pp. 1–92, May 2014, doi: 10.1002/14356007.A18_545.PUB4.

[19] J. Sun, M. Zhao, L. Huang, T. Zhang, and Q. Wang, "Recent progress on direct air capture of carbon dioxide," *Curr Opin Green Sustain Chem*, vol. 40, p. 100752, Apr. 2023, doi: 10.1016/J.COGSC.2023.100752.

[20] S. Kumar, R. Srivastava, and J. Koh, "Utilization of zeolites as CO2 capturing agents: Advances and future perspectives," *Journal of CO2 Utilization*, vol. 41, p. 101251, Oct. 2020, doi: 10.1016/J.JCOU.2020.101251.

[21] C. A. Trickett, A. Helal, B. A. Al-Maythalony, Z. H. Yamani, K. E. Cordova, and O. M. Yaghi, "The chemistry of metal–organic frameworks for CO2 capture, regeneration and conversion," *Nature Reviews Materials 2017 2:8*, vol. 2, no. 8, pp. 1–16, Jul. 2017, doi: 10.1038/natrevmats.2017.45.

[22] R. Krishna and J. M. Van Baten, "A comparison of the CO2 capture characteristics of zeolites and metal–organic frameworks," *Sep Purif Technol*, vol. 87, pp. 120–126, Mar. 2012, doi: 10.1016/J.SEPPUR.2011.11.031.

[23] S. A. Didas, S. Choi, W. Chaikittisilp, and C. W. Jones, "Amine-Oxide Hybrid Materials for CO2 Capture from Ambient Air," *Acc Chem Res*, vol. 48, no. 10, pp. 2680–2687, Oct. 2015, doi: 10.1021/ACS.ACCOUNTS.5B00284/SUPPL_FILE/AR5B00284_SI_001.PDF.

[24] C. G. Piscopo and S. Loebbecke, "Strategies to Enhance Carbon Dioxide Capture in Metal-Organic Frameworks," *Chempluschem*, vol. 85, no. 3, pp. 538–547, Mar. 2020, doi: 10.1002/CPLU.202000072.

[25] X. Zhu *et al.*, "Efficient CO2 capture from ambient air with amine-functionalized Mg–Al mixed metal oxides," *J Mater Chem A Mater*, vol. 8, no. 32, pp. 16421–16428, Aug. 2020, doi: 10.1039/D0TA05079B.

[26] S. Fujikawa and R. Selyanchyn, "Direct air capture by membranes," *MRS Bull*, vol. 47, no. 4, pp. 416–423, Apr. 2022, doi: 10.1557/S43577-022-00313-6/FIGURES/6.

[27] R. Castro-Muñoz, M. Zamidi Ahmad, M. Malankowska, and J. Coronas, "A new relevant membrane application: CO2 direct air capture (DAC)," *Chemical Engineering Journal*, vol. 446, p. 137047, Oct. 2022, doi: 10.1016/J.CEJ.2022.137047.

[28] L. R. López *et al.*, "CO2 in indoor environments: From environmental and health risk to potential renewable carbon source," *Science of The Total Environment*, vol. 856, p. 159088, Jan. 2023, doi: 10.1016/J.SCITOTENV.2022.159088.

[29] C. Wang, H. Liu, X. Li, and L. Zheng, "Importance of ambient O2 for electrochemical enrichment of atmospheric CO2," *Ind Eng Chem Res*, vol. 52, no. 7, pp. 2470–2476, Feb. 2013, doi: 10.1021/IE302991Y/SUPPL_FILE/IE302991Y_SI_001.PDF.

[30] A. M. Zito *et al.*, "Electrochemical Carbon Dioxide Capture and Concentration," *Chem Rev*, vol. 123, no. 13, pp. 8069–8098, Jul. 2023, doi: 10.1021/ACS.CHEMREV.2C00681/ASSET/IMAGES/MEDIUM/CR2C00681_0018.GIF.

[31] W. Ye *et al.*, "Environmental evaluation of bipolar membrane electrodialysis for NaOH production from wastewater: Conditioning NaOH as a CO2 absorbent," *Sep Purif Technol*, vol. 144, pp. 206–214, Apr. 2015, doi: 10.1016/J.SEPPUR.2015.02.031.

[32] M. Wang, S. Hariharan, R. A. Shaw, and T. A. Hatton, "Energetics of electrochemically mediated amine regeneration process for flue gas CO2 capture," *International Journal of Greenhouse Gas Control*, vol. 82, pp. 48–58, Mar. 2019, doi: 10.1016/J.IJGGC.2018.12.028.

[33] J. M. Barlow *et al.*, "Molecular design of redox carriers for electrochemical CO2 capture and concentration," *Chem Soc Rev*, vol. 51, no. 20, pp. 8415–8433, Oct. 2022, doi: 10.1039/D2CS00367H.

[34] M. Ozkan, S. P. Nayak, A. D. Ruiz, and W. Jiang, "Current status and pillars of direct air capture technologies," *iScience*, vol. 25, no. 4, p. 103990, Apr. 2022, doi: 10.1016/J.ISCI.2022.103990/ASSET/E80BEE23-20F5-43E6-943C-8BFE0CAA311C/MAIN.ASSETS/GR8.JPG.

[35] M. Erans, E. S. Sanz-Pérez, D. P. Hanak, Z. Clulow, D. M. Reiner, and G. A. Mutch, "Direct air capture: process technology, techno-economic and socio-political challenges," *Energy Environ Sci*, vol. 15, no. 4, pp. 1360–1405, Apr. 2022, doi: 10.1039/D1EE03523A.

[36] "Carbon Engineering | Direct Air Capture of CO2 | Home." Accessed: Mar. 16, 2025. [Online]. Available: https://carbonengineering.com/

[37] C. Kurt and J. Bittner, "Sodium Hydroxide," *Ullmann's Encyclopedia of Industrial Chemistry*, Jul. 2006, doi: 10.1002/14356007.A24_345.PUB2.

[38] K. An, A. Farooqui, and S. T. McCoy, "The impact of climate on solvent-based direct air capture systems," *Appl Energy*, vol. 325, p. 119895, Nov. 2022, doi: 10.1016/J.APENERGY.2022.119895.

[39] K. Ebner, L. Koops, L. Moser, and A. Sizmann, “Direct Air Capture,” *Green Energy and Technology*, vol. Part F3771, pp. 431–450, 2025, doi: 10.1007/978-3-031-62411-7_16.

[40] “Getting Started Guides | Latest AspenTech Software Releases | Installation, Support & More.” Accessed: May 19, 2025. [Online]. Available: https://www.aspentech.com/en/getting-started-guides

[41] M. Mostafa, C. Antonicelli, C. Varela, D. Barletta, and E. Zondervan, “Capturing CO2 from the atmosphere: Design and analysis of a large-scale DAC facility,” *Carbon Capture Science & Technology*, vol. 4, p. 100060, Sep. 2022, doi: 10.1016/J.CCST.2022.100060.

[42] V. B. Seithümmer, C. Dubiel, S. J. Kaufmann, H. Chinnaraj, P. Rößner, and K. P. Birke, “Direct Air Capture via Counter-Current NaOH Absorption System: Evolution of pH for Subsequent Plasma-Enhanced CO_2 Utilization,” *Chemie Ingenieur Technik*, vol. 97, no. 5, pp. 554–559, May 2025, doi: 10.1002/CITE.202400145.

[43] J. Liu *et al.*, “Hydrogen-motivated electrolysis of sodium carbonate with extremely low cell voltage,” *Chemical Communications*, vol. 54, no. 29, pp. 3582–3585, 2018, doi: 10.1039/C8CC00812D,.

[44] G. Holmes and D. W. Keith, “An air–liquid contactor for large-scale capture of CO2 from air,” *Philosophical Transactions of the Royal Society A: Mathematical, Physical and Engineering Sciences*, vol. 370, no. 1974, pp. 4380–4403, Sep. 2012, doi: 10.1098/RSTA.2012.0137.

[45] F. Sabatino *et al.*, “Evaluation of a Direct Air Capture Process Combining Wet Scrubbing and Bipolar Membrane Electrodialysis,” *Ind Eng Chem Res*, vol. 59, no. 15, pp. 7007–7020, Apr. 2020, doi: 10.1021/ACS.IECR.9B05641/ASSET/IMAGES/LARGE/IE9B05641_0013.JPEG.

[46] V. Spallina, D. Pandolfo, A. Battistella, M. C. Romano, M. Van Sint Annaland, and F. Gallucci, “Techno-economic assessment of membrane assisted fluidized bed reactors for pure H2 production with CO2 capture,” *Energy Convers Manag*, vol. 120, pp. 257–273, Jul. 2016, doi: 10.1016/J.ENCONMAN.2016.04.073.

[47] K. Gerdes, W. M. Summers, and J. Wimer, “Quality Guidelines for Energy System Studies: Cost Estimation Methodology for NETL Assessments of Power Plant Performance,” Aug. 2011, doi: 10.2172/1513278.

[48] J. K. Stolaroff, D. W. Keith, and G. V. Lowry, "Carbon dioxide capture from atmospheric air using sodium hydroxide spray," *Environ Sci Technol*, vol. 42, no. 8, pp. 2728–2735, Apr. 2008, doi: 10.1021/ES702607W/SUPPL_FILE/ES702607W-FILE007.PDF.

[49] A. Franco and C. Giovannini, "Recent and Future Advances in Water Electrolysis for Green Hydrogen Generation: Critical Analysis and Perspectives," *Sustainability 2023, Vol. 15, Page 16917*, vol. 15, no. 24, p. 16917, Dec. 2023, doi: 10.3390/SU152416917.

[50] D. W. Keith, G. Holmes, D. St. Angelo, and K. Heidel, "A Process for Capturing CO2 from the Atmosphere," *Joule*, vol. 2, no. 8, pp. 1573–1594, Aug. 2018, doi: 10.1016/j.joule.2018.05.006.

[51] K. Heidel, D. Keith, A. Singh, and G. Holmes, "Process design and costing of an air-contactor for air-capture," *Energy Procedia*, vol. 4, pp. 2861–2868, Jan. 2011, doi: 10.1016/J.EGYPRO.2011.02.192.

[52] V. Spallina, D. Pandolfo, A. Battistella, M. C. Romano, M. Van Sint Annaland, and F. Gallucci, "Techno-economic assessment of membrane assisted fluidized bed reactors for pure H2 production with CO2 capture," *Energy Convers Manag*, vol. 120, pp. 257–273, Jul. 2016, doi: 10.1016/J.ENCONMAN.2016.04.073.

[53] K. Gerdes, W. M. Summers, and J. Wimer, "Quality Guidelines for Energy System Studies: Cost Estimation Methodology for NETL Assessments of Power Plant Performance," Aug. 2011, doi: 10.2172/1513278.

[54] F. Sabatino *et al.*, "Evaluation of a Direct Air Capture Process Combining Wet Scrubbing and Bipolar Membrane Electrodialysis," *Ind Eng Chem Res*, vol. 59, no. 15, pp. 7007–7020, Apr. 2020, doi: 10.1021/ACS.IECR.9B05641/ASSET/IMAGES/LARGE/IE9B05641_0013.JPEG.

[55] "Global average levelised cost of hydrogen production by energy source and technology, 2019 and 2050 – Charts – Data & Statistics - IEA." Accessed: May 28, 2025. [Online]. Available: https://www.iea.org/data-and-statistics/charts/global-average-levelised-cost-of-hydrogen-production-by-energy-source-and-technology-2019-and-2050

[56] "U.S. National Hydrogen Strategy and Roadmap | Hydrogen Program." Accessed: May 28, 2025. [Online]. Available: https://www.hydrogen.energy.gov/library/roadmaps-vision/clean-hydrogen-strategy-roadmap

[57] "How Many Watts Does A Laptop Use - 1,084 Studied | With Data." Accessed: Apr. 17, 2025. [Online]. Available: https://ecocostsavings.com/how-many-watts-does-a-laptop-use/

[58] "EPREL Public website." Accessed: Apr. 17, 2025. [Online]. Available: https://eprel.ec.europa.eu/screen/product/electronicdisplays/1923365

[59] "How Much Electricity Does a PC Consume? - ComputerCity." Accessed: Apr. 17, 2025. [Online]. Available: https://computercity.com/hardware/psus/how-much-electricity-does-a-pc-consume

[60] "The Hidden Environmental Costs of Chat GPTs: A Conversation with Bing Copilot - Bylines Scotland." Accessed: Apr. 17, 2025. [Online]. Available: https://bylines.scot/environment/environmental-costs-of-chat-gtps/

[61] "Carbon intensity of electricity generation, 2023." Accessed: Apr. 17, 2025. [Online]. Available: https://ourworldindata.org/grapher/carbon-intensity-electricity

[62] "Emission Factor: International short-haul flight economy - with RF effect | Transport | Air Travel | United Kingdom | Climatiq." Accessed: Apr. 17, 2025. [Online]. Available: https://www.climatiq.io/data/emission-factor/6053c057-3814-42a1-a73c-f94f8f06c69c

[63] "THE 17 GOALS | Sustainable Development." Accessed: Apr. 17, 2025. [Online]. Available: https://sdgs.un.org/goals